

不稳定原子核的奇特结构与直接 反应机制研究

王建松

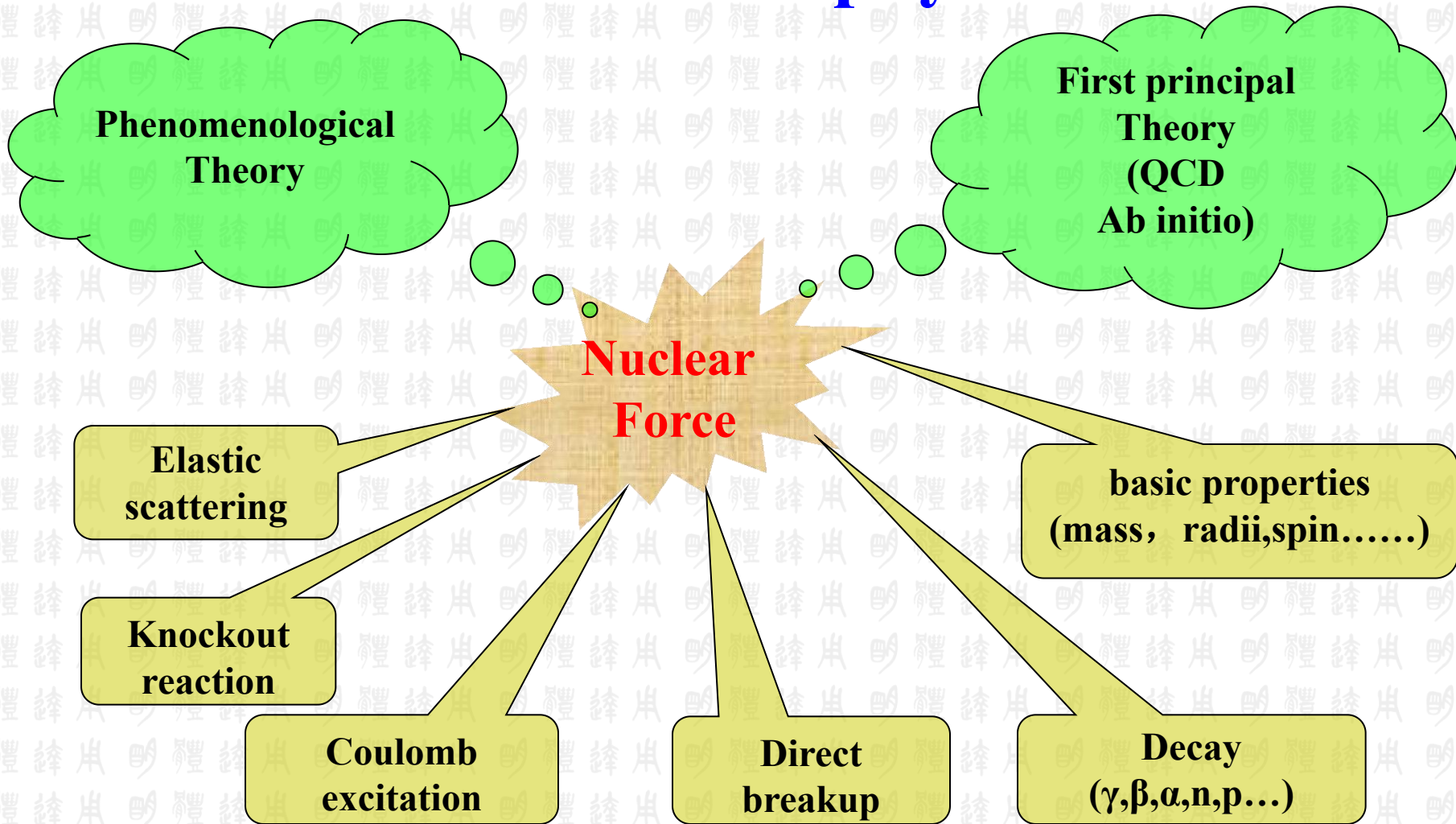
湖州师范学院



报告内容

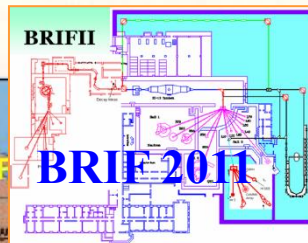
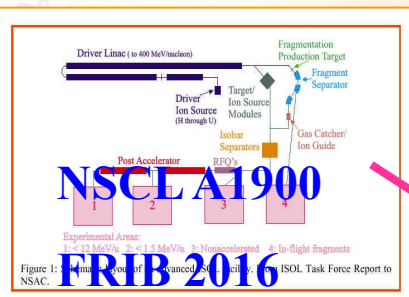
- 不稳定原子核研究背景：晕结构
- 不稳定原子核的奇特结构与直接反应
- 原子核的3核子集团 (t 、 ${}^3\text{He}$) 和纯中子集团
- 结论和展望

What does nuclear physics do?

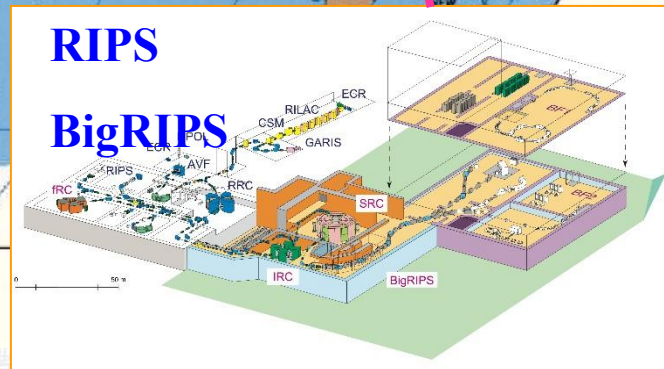
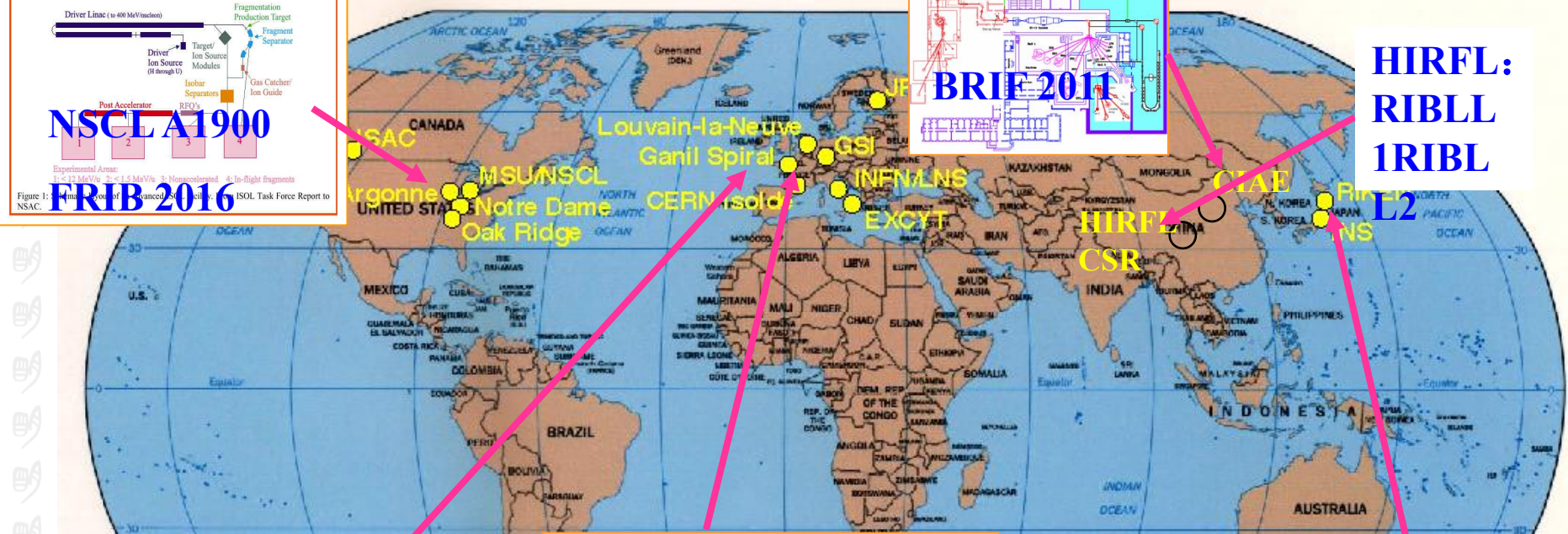


The **precise** and **accurate** experimental data is the benchmark

国内外核物理实验大科学装置



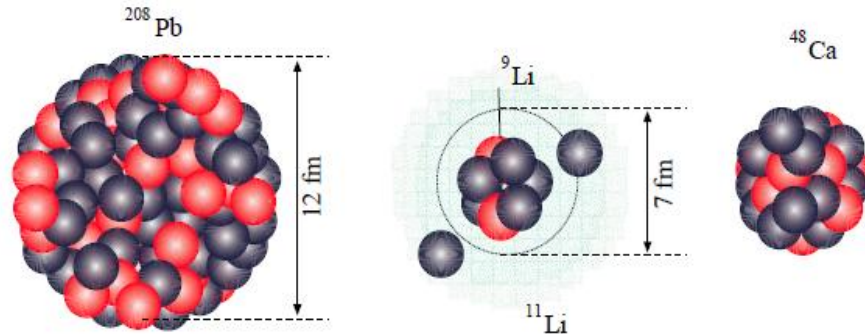
**HIRFL:
RIBLL
1RIBL**



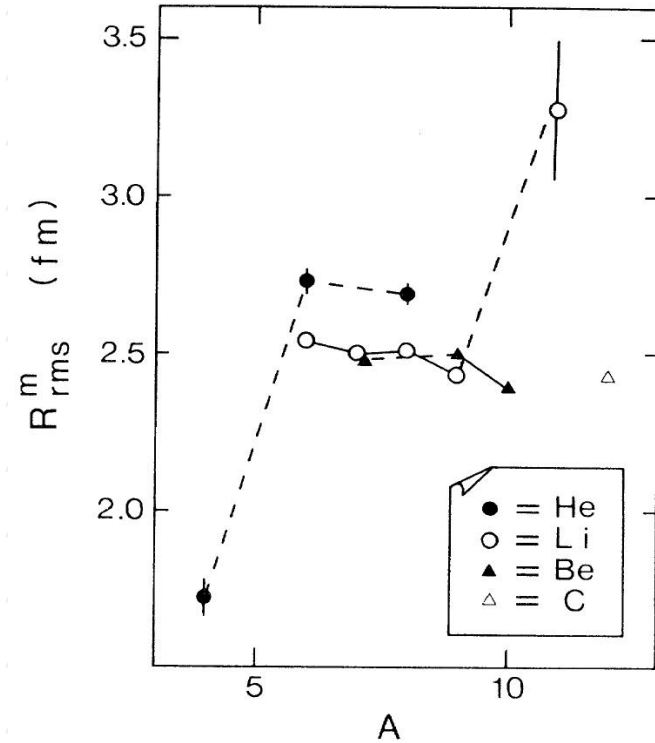
原子核晕结构的发现

 TABLE I. Interaction cross sections (σ_I) in millibarns.

Beam	Be	Target C	Al
^6Li	651 ± 6	688 ± 10	1010 ± 11
^7Li	686 ± 4	736 ± 6	1071 ± 7
^8Li	727 ± 6	768 ± 9	1147 ± 14
^9Li	739 ± 5	796 ± 6	1135 ± 7
^{11}Li		1040 ± 60	
^7Be	682 ± 6	738 ± 9	1050 ± 17
^9Be	755 ± 6	806 ± 9	1174 ± 11
^{10}Be	755 ± 7	813 ± 10	1153 ± 16



Phys.Rep.389,1-59



I. Tanihata et al., PRL55(1985)2676



晕结构存在的条件

- 价核子处于s或p轨道
- 价核子的分离能很小

$$B < 270 \text{ keV} \frac{A^2}{Z^2} \text{ for } s\text{-states,} \quad (9)$$

$$Z < 0.44 A^{4/3} \text{ for } p\text{-states,} \quad (10)$$

$$B < 2 \text{ MeV } A^{-2/3} \text{ for both } s\text{- and } p\text{-states,} \quad (11)$$

A.S. Jensen, K. Riisager, Physics Letters B 480 (2000) 39–44



s,p轨道不是晕核存在的必要条件?

PHYSICAL REVIEW LETTERS **126**, 082501 (2021)

Quasifree Neutron Knockout Reaction Reveals a Small *s*-Orbital Component in the Borromean Nucleus ^{17}B

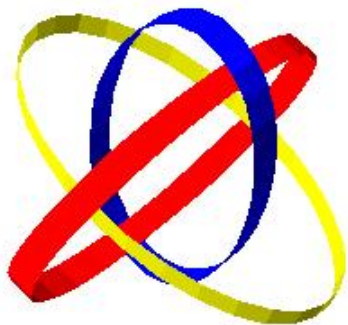
Z. H. Yang^{1,2,*} Y. Kubota^{2,3,†} A. Corsi,⁴ K. Yoshida,⁵ X.-X. Sun,^{6,7} J. G. Li,⁸ M. Kimura,^{9,10,1} N. Michel,^{11,12} K. Ogata,^{1,13} C. X. Yuan,¹⁴ Q. Yuan,⁸ G. Authelet,⁴ H. Baba,² C. Caesar,¹⁵ D. Calvet,⁴ A. Delbart,⁴ M. Dozono,³ J. Feng,⁸ F. Flavigny,^{16,‡} J.-M. Gheller,⁴ J. Gibelin,¹⁷ A. Giganon,⁴ A. Gillibert,⁴ K. Hasegawa,¹⁸ T. Isobe,² Y. Kanaya,¹⁹ S. Kawakami,¹⁹ D. Kim,²⁰ Y. Kiyokawa,³ M. Kobayashi,³ N. Kobayashi,²¹ T. Kobayashi,¹⁸ Y. Kondo,²² Z. Korkulu,^{20,23} S. Koyama,²¹ V. Lapoux,⁴ Y. Maeda,¹⁹ F. M. Marqués,¹⁷ T. Motobayashi,² T. Miyazaki,²¹ T. Nakamura,²² N. Nakatsuka,²⁴ Y. Nishio,²⁵ A. Obertelli,^{4,†} A. Ohkura,²⁵ N. A. Orr,¹⁷ S. Ota,³ H. Otsu,² T. Ozaki,²² V. Panin,² S. Paschalis,^{15,§} E. C. Pollacco,⁴ S. Reichert,²⁶ J.-Y. Roussé,⁴ A. T. Saito,²² S. Sakaguchi,²⁵ M. Sako,² C. Santamaria,⁴ M. Sasano,² H. Sato,² M. Shikata,²² Y. Shimizu,² Y. Shindo,²⁵ L. Stuhl,^{20,2} T. Sumikama,¹⁸ Y. L. Sun,^{4,†} M. Tabata,²⁵ Y. Togano,^{22,27} J. Tsubota,²² F. R. Xu,⁸ J. Yasuda,²⁵

谱因子数据表明: **s** 波只占 **9%**, 其余为**d**波

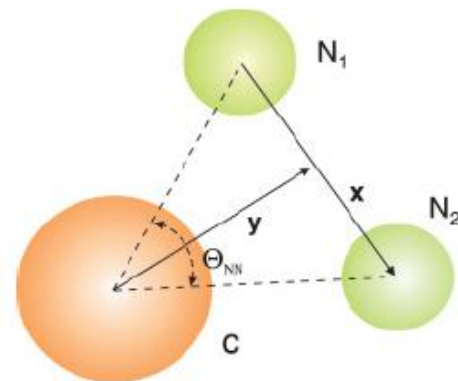
explained by the deformed relativistic Hartree-Bogoliubov theory in continuum, revealing a definite but not dominant neutron halo in ^{17}B . The present work gives the smallest *s*- or *p*-orbital component among known nuclei exhibiting halo features and implies that the dominant occupation of *s* or *p* orbitals is not a prerequisite for the occurrence of a neutron halo.



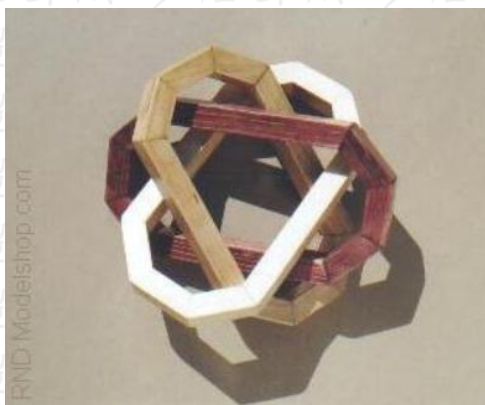
Borromean Nuclei ${}^6\text{He}$



point-proton radius of ${}^6\text{He}$: **1.912 ± 0.018 fm**



L. -B. Wang et al., PhysRevLett.93.142501(2004)



- o PRL 117, 222501 (2016) “How Many-Body Correlations and α Clustering Shape ${}^6\text{He}$ ”
- o The simultaneous reproduction of its small binding energy and extended matter and point-proton radii has been a challenge for ab initio theoretical calculations based on traditional bound-state methods

理论预言可能的奇特晕结构

巨晕核
核芯形变

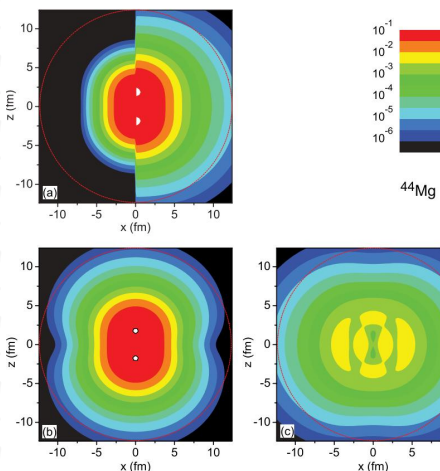
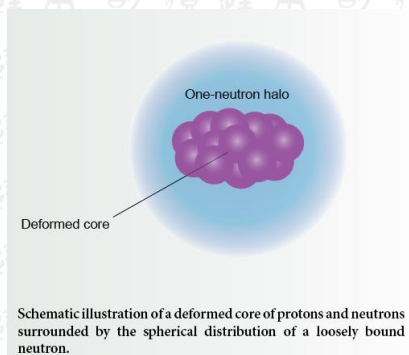
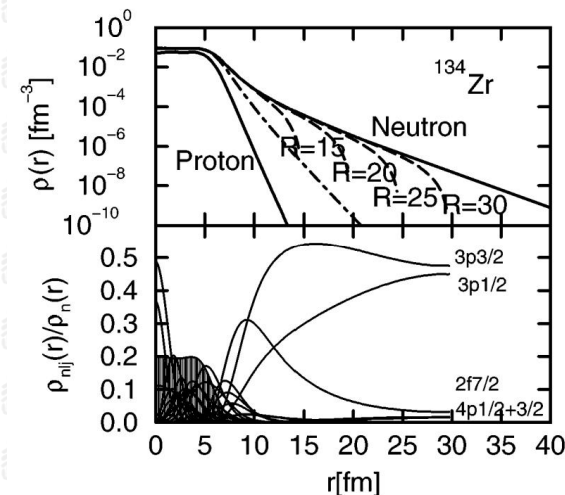
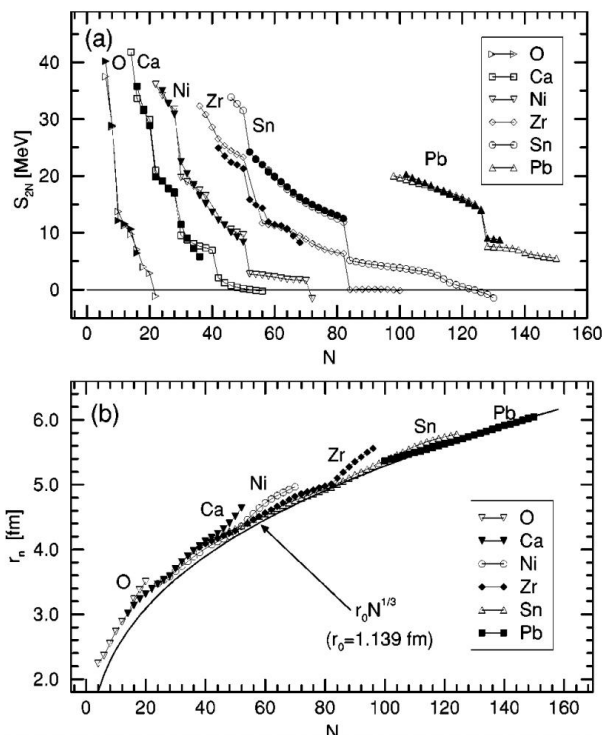


FIG. 1. (Color online) Density distributions of ⁴⁴Mg with the z axis as the symmetry axis. (a) The proton density (for x < 0) and the neutron density (for x > 0), (b) the density of the neutron core, and (c) the density of the neutron halo. In each plot, a dotted circle is drawn to guide the eye.



J. Meng and P. Ring, Phys. Rev. Lett. **80**, 460 (1998) cited 238 times/J. Meng et al., Phys. Rev. C **65**(2002) 041302(R) /Phys. Rev. **74**, 054318 (2006)

S. G. Zhou, J. Meng, Phys. Rev. C **82**, 011301(R) (2010) cited 139 times

Light Halo Nuclei

³⁹Na



¹⁷ Ne	¹⁸ Ne	¹⁹ Ne	²⁰ Ne	²¹ Ne	²² Ne	²³ Ne	²⁴ Ne	²⁵ Ne	²⁶ Ne	²⁷ Ne	²⁸ Ne	²⁹ Ne	³⁰ Ne	³¹ Ne	³² Ne	³⁴ Ne
	¹⁷ F	¹⁸ F	¹⁹ F	²⁰ F	²¹ F	²² F	²³ F	²⁴ F	²⁵ F	²⁶ F	²⁷ F		²⁹ F		³¹ F	

		¹³ O	¹⁴ O	¹⁵ O	¹⁶ O	¹⁷ O	¹⁸ O	¹⁹ O	²⁰ O	²¹ O	²² O	²³ O	²⁴ O		
		¹² N	¹³ N	¹⁴ N	¹⁵ N	¹⁶ N	¹⁷ N	¹⁸ N	¹⁹ N	²⁰ N	²¹ N	²² N	²³ N		
	⁹ C	¹⁰ C	¹¹ C	¹² C	¹³ C	¹⁴ C	¹⁵ C	¹⁶ C	¹⁷ C	¹⁸ C	¹⁹ C	²⁰ C		²² C	
	⁸ B		¹⁰ B	¹¹ B	¹² B	¹³ B	¹⁴ B	¹⁵ B		¹⁷ B		¹⁹ B			
	⁷ Be		⁹ Be	¹⁰ Be	¹¹ Be	¹² Be	¹³ Be	¹⁴ Be							
	⁶ Li	⁷ Li	⁸ Li	⁹ Li		¹¹ Li									
	³ He	⁴ He		⁶ He		⁸ He									
¹ H	² H	³ H													
	¹ n														

PRL123 (2019) 212501
PRL123 (2022) 212502



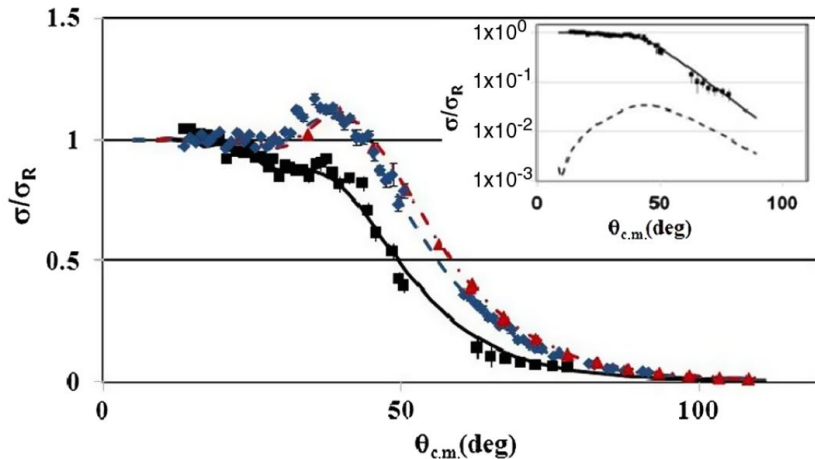
	Sp /S2p(MeV)		Sn (MeV)
⁸ B	0.136	⁶ He	0.976(2n)
⁹ C	1.300	⁸ He	3.1 (4n)
¹² N	0.600	¹¹ Li	0.369(2n)
¹³ O	1.512	¹¹ Be	0.502
¹⁷ F	0.600	¹⁴ Be	1.266 (2n)
¹⁷ Ne	0.933 (2p)	¹⁷ B	1.385
		¹⁹ C	0.577

⁸B: S_p = 136.4 keV 10, T_{1/2} = 770 ms 3
found in 1950 at Berkley linear accelerator

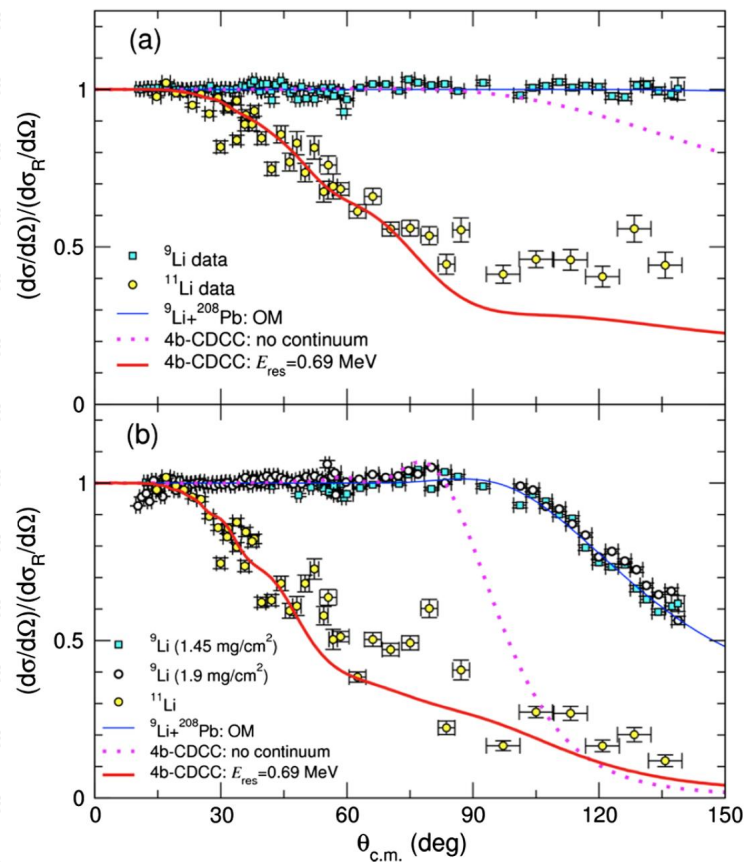
中子晕核 ^{11}Be 、 ^{11}Li 对弹性散射的影响

9、 $^{11}\text{Li}+^{208}\text{Pb}$

9、10、 $^{11}\text{Be}+^{64}\text{Zn}$



A. Di Pietro et al., PRL 105 (2010) 022701
@REX-ISOLDE at CERN



M. Cubero et al., PRL 109 (2012) 262701 @TRIUMF

^{11}Be 在 ^{197}Au 靶上的核心激发效应

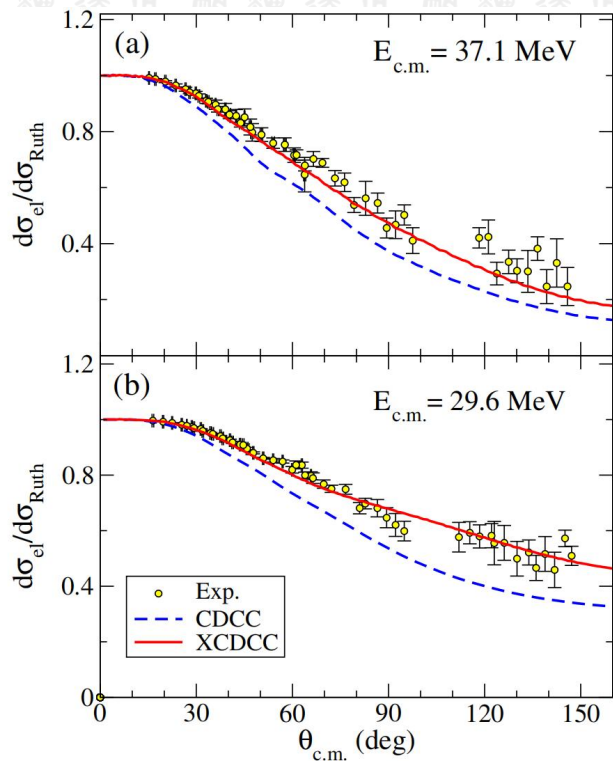


FIG. 3. Measured differential elastic scattering cross sections (a) $E_{c.m.} = 37.1$ MeV and (b) 29.6 MeV, compared with CDCC and XCDCC calculations described in the text.

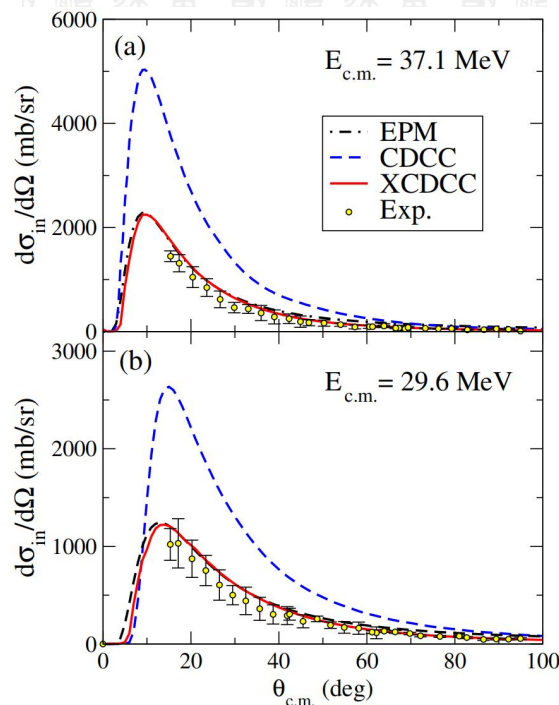


FIG. 4. Measured and calculated angular distribution of the inelastic differential cross section of $^{11}\text{Be} + ^{197}\text{Au}$, populating the $1/2^-$ bound excited state in ^{11}Be for (a) $E_{c.m.} = 37.1$ MeV and (b) 29.6 MeV. The curves are the EPM, CDCC, and XCDCC calculations described in the text.

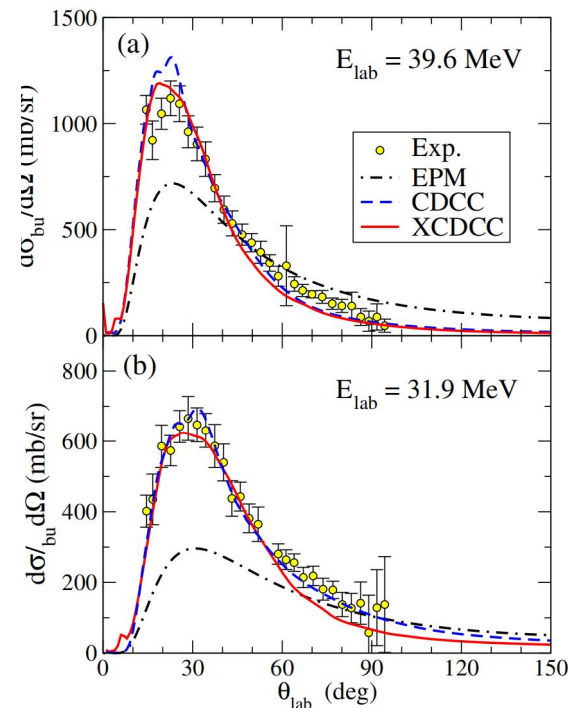
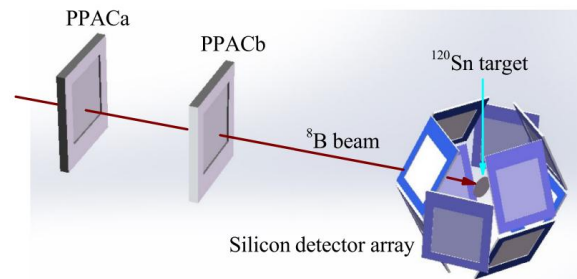
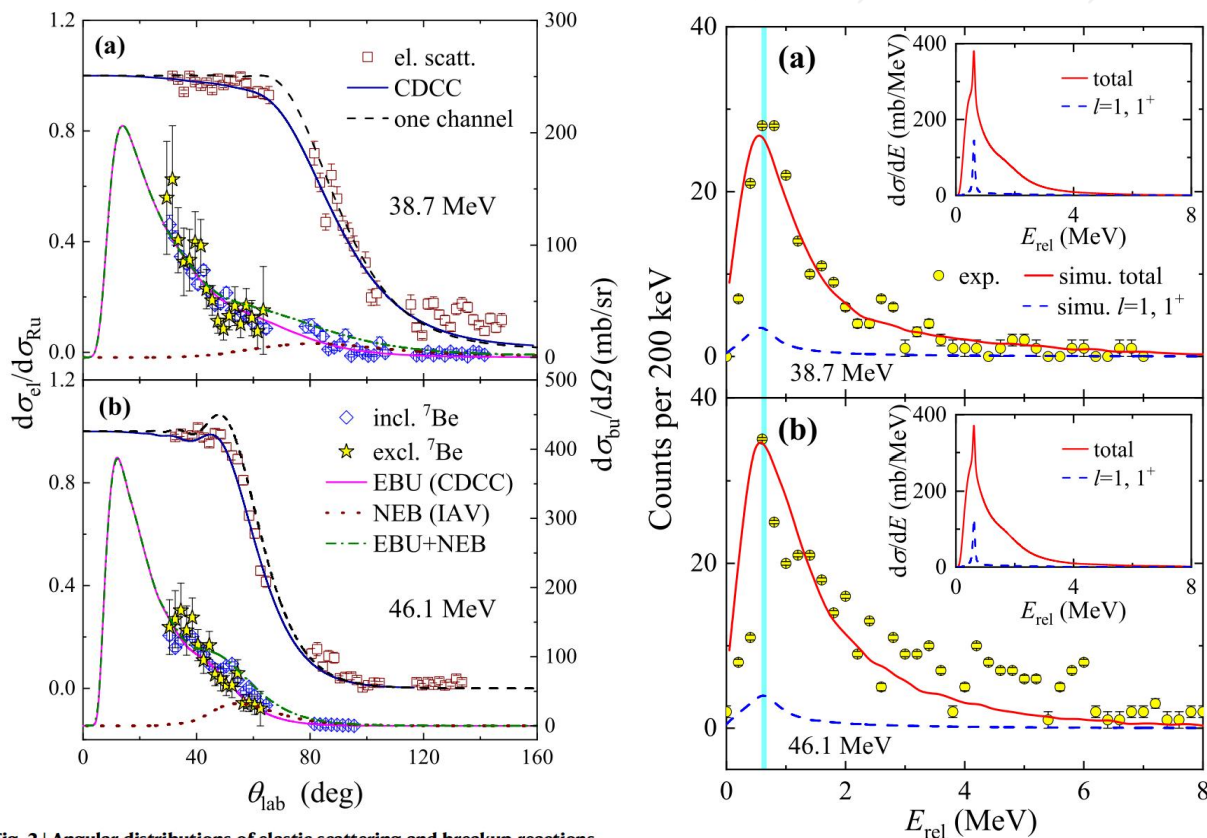


FIG. 5. Experimental differential breakup cross section in the laboratory frame at (a) $E_{lab} = 39.6$ MeV and (b) 31.9 MeV, compared with EPM, CDCC, and XCDCC calculations described in the text.

V. Pesudo, M. J. G. Borge, A. M. Moro et al., PRL 118, 152502 (2017) @ TRIUMF

^8B 在库仑位垒附近的破裂机制研究



- ◆ ^8B 具有与 ^6He 等中子晕核不一样的反应机制,
- ◆ 破裂反应对弹性散射和完全融合反应影响不显著。

Fig. 2 | Angular distributions of elastic scattering and breakup reactions.

Squares, diamonds and stars denote the experimental data of elastic scattering, Fig. 3 | Measured E_{rel} distributions for breakup fragments ^7Be and proton. The inclusive and exclusive breakup at a 38.7 and b 46.1 MeV, respectively. The elast experimental data (circles) at a 38.7 and b 46.1 MeV are compared with the simu-

L. Yang C. J. Lin ..., *JW*, Nature Communications(2022)13:7193

不稳定原子核的奇特结构与直接反应

早期在RIBLL开展不稳定核弹性散射研究

第26卷第6期

高能物理与核物理

Vol. 26, No. 6

2002年6月

HIGH ENERGY PHYSICS AND NUCLEAR PHYSICS

Jun., 2002

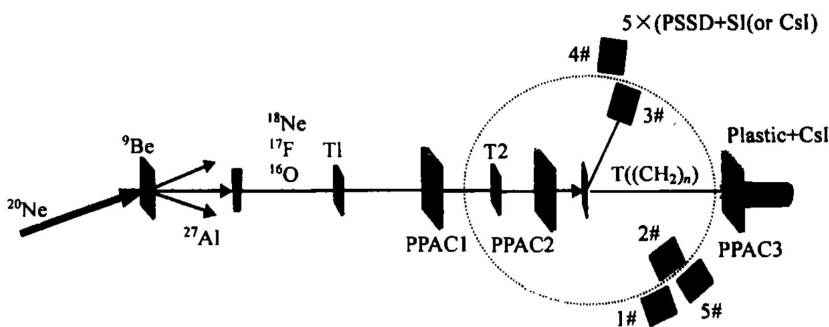
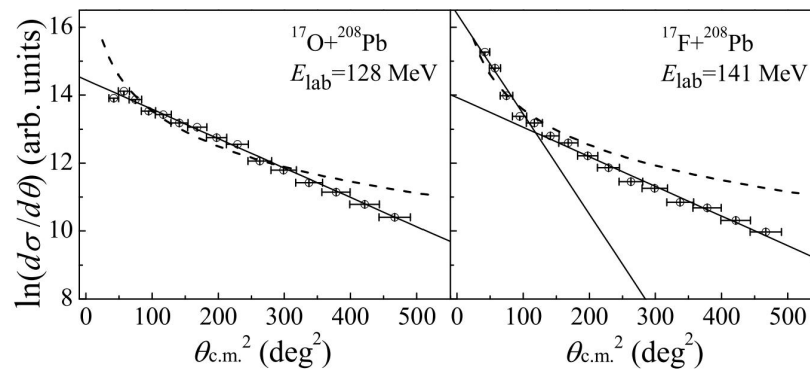
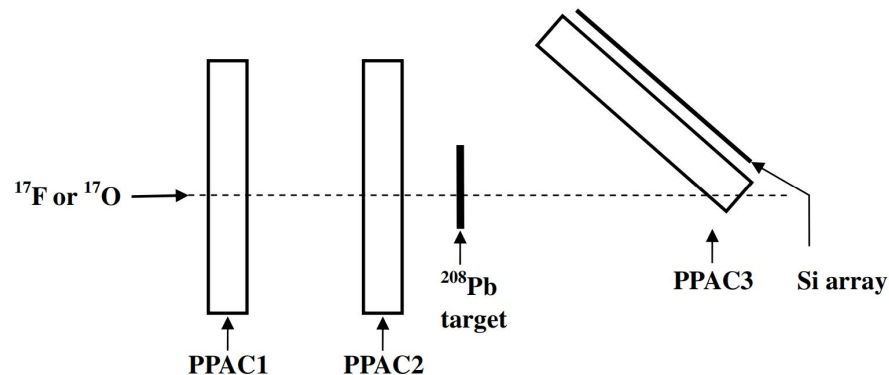
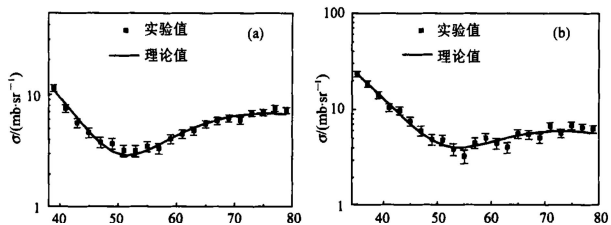
^{17}F 和 ^{18}Ne 与质子的弹性散射角分布 *

卢朝晖 吴和宇 胡荣江 诸永泰 张保国 李祖玉 魏志勇
段利敏 王宏伟 肖志刚 王素芳 靳根明 郭忠言
肖国青 朱海东 柳永英 陈克良

(中国科学院近代物理研究所 兰州 730000)

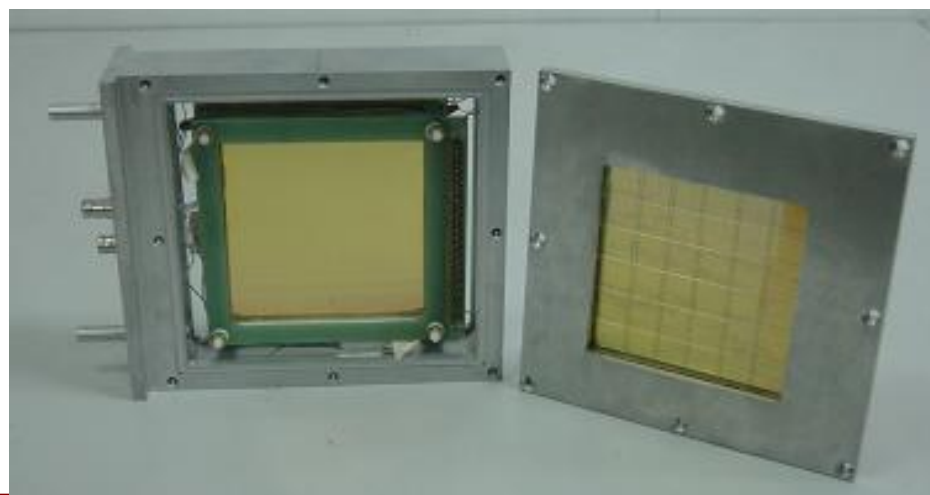
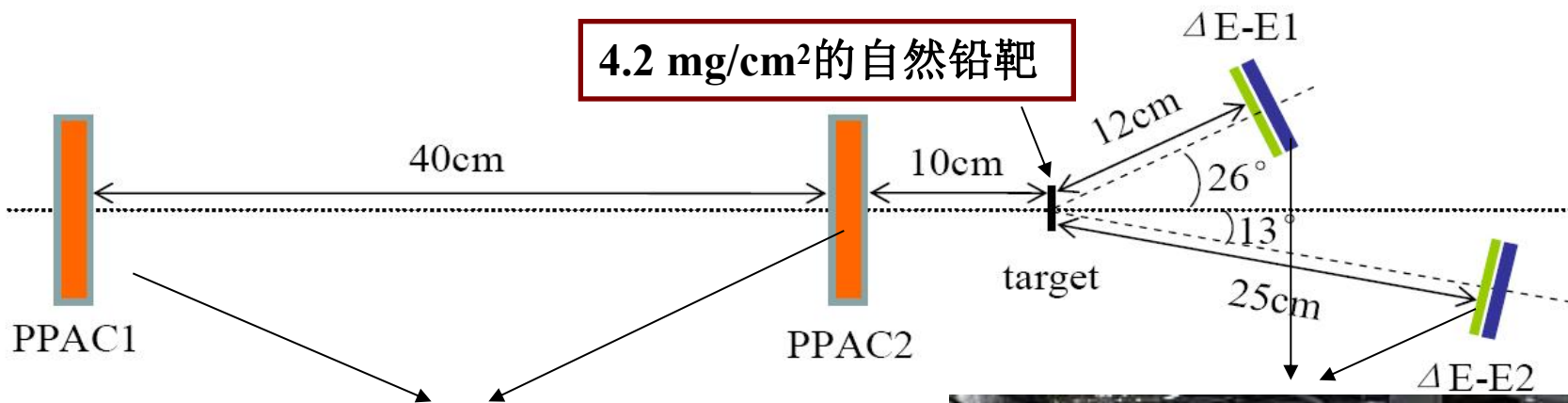
陈陶 李湘庆 李智焕

(北京大学技术物理系 北京 100871)



白真, 王琦, 韩建龙等
Chinese Physics Letters 24, 3384

探测器布局



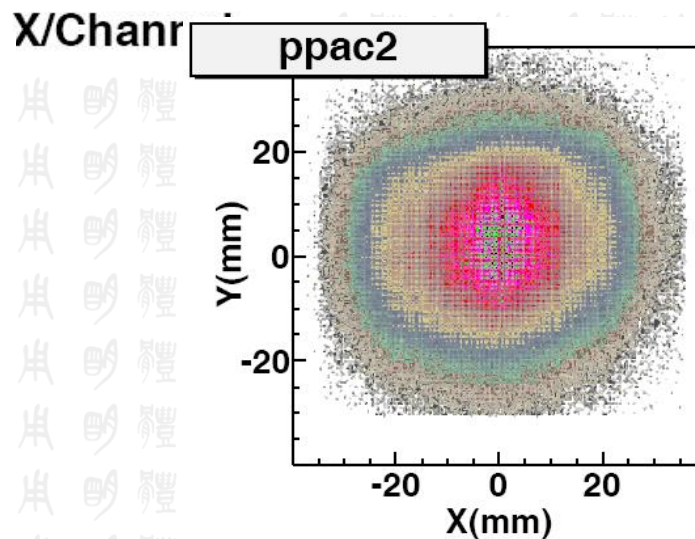
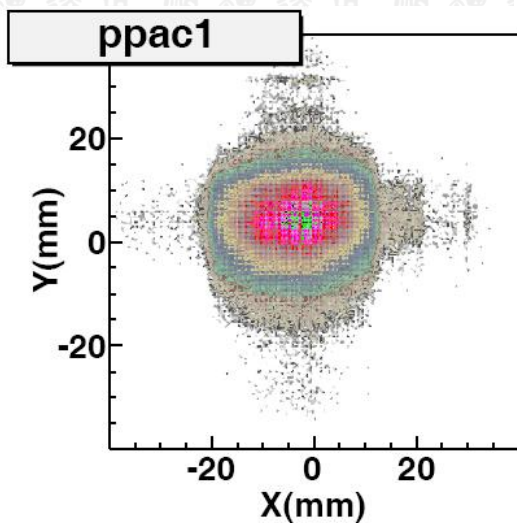
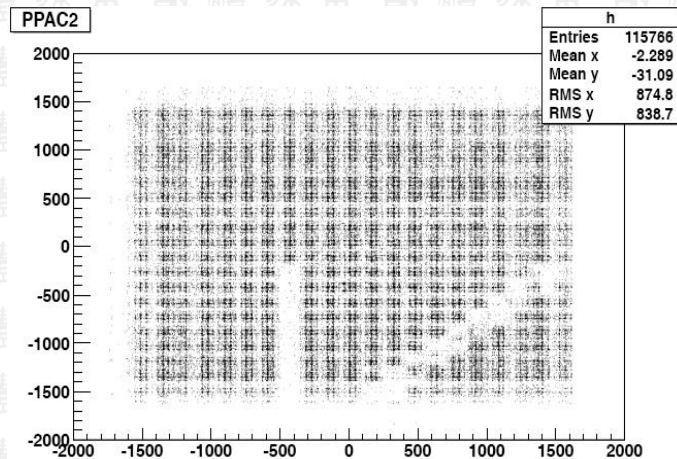
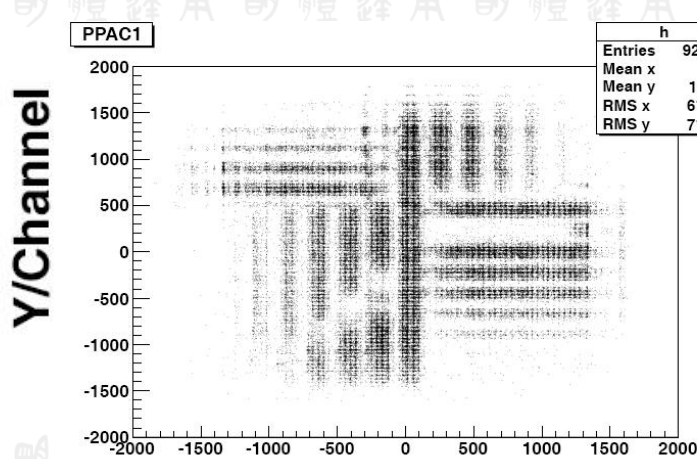
- ❖ PPAC灵敏面积为 $80 \times 80 \text{ mm}^2$, 采用延迟块读出。
- ❖ 位置分辨为1 mm。
- ❖ 在PPAC上也会散射。

ΔE : $48 \times 48 \text{ mm}^2$, $150 \mu\text{m}$
DSSD (48+48)

E: $50 \times 50 \text{ mm}^2$ $1500 \mu\text{m}$ SSD

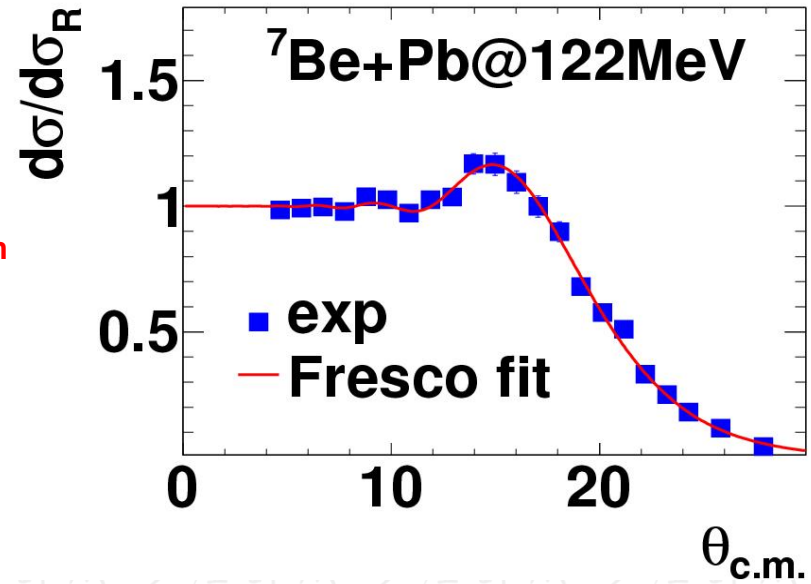
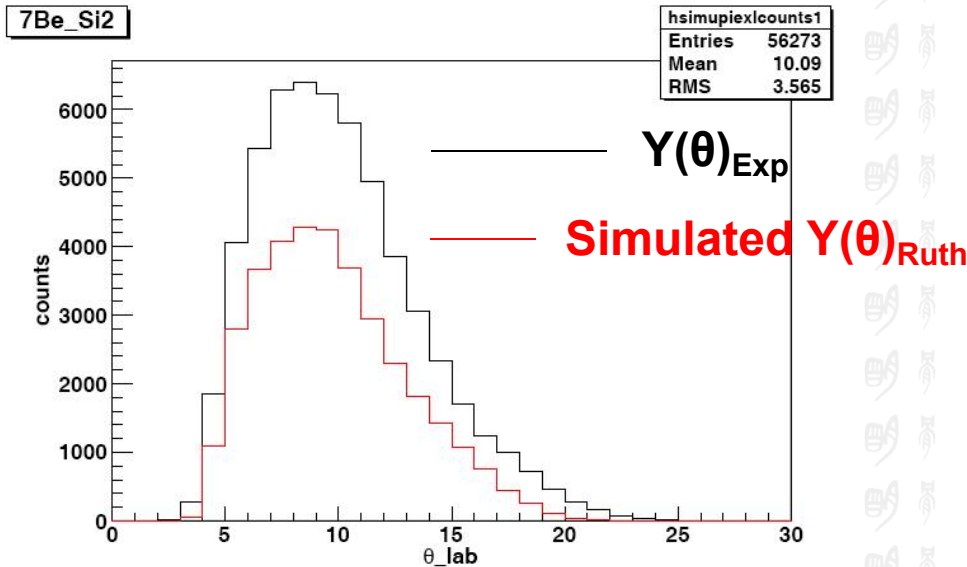
能量分辨 (α 源): 0.5 - 0.9% DSSD
1.2%-1.3% SSD

PPAC的位置刻度





How to Obtain the Correct ES Angular Distribution

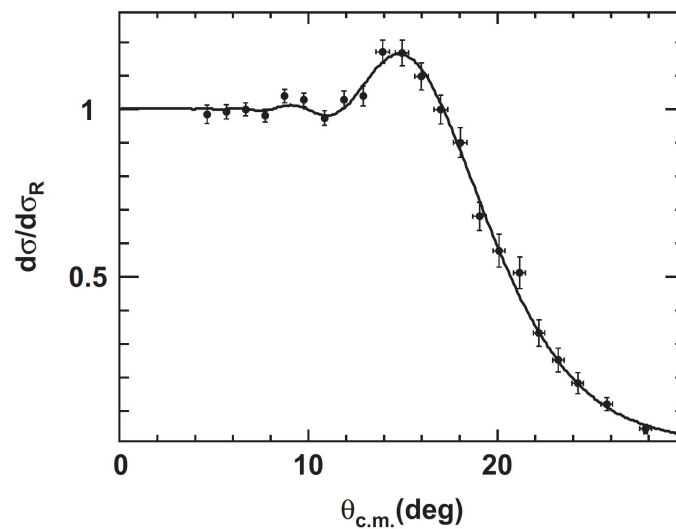
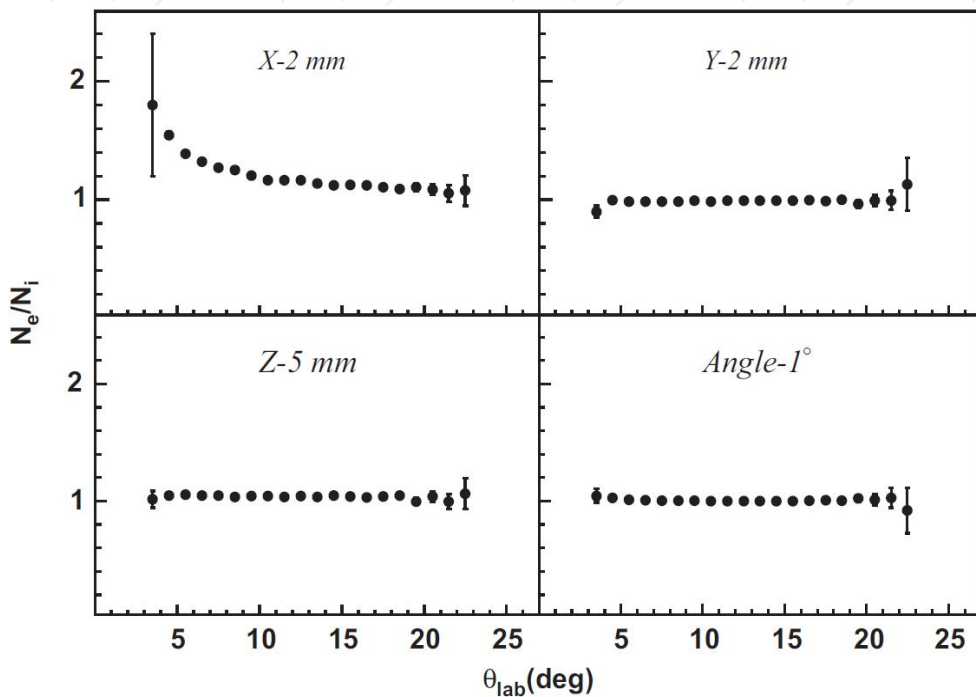
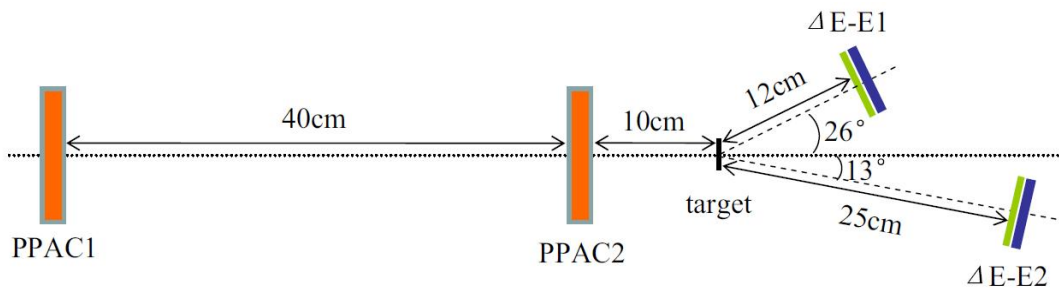


Because the secondary beams are dispersed widely, we have to simulate the Rutherford scattering events and compare with the experimental data to obtain the normalized differential cross section as the following:

$$\sigma/\sigma_{\text{Ruth}}(\theta) = Y(\theta)_{\text{Exp}}/Y(\theta)_{\text{Sim}}$$

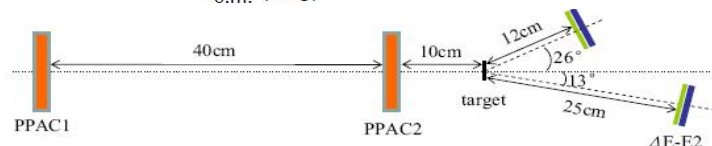
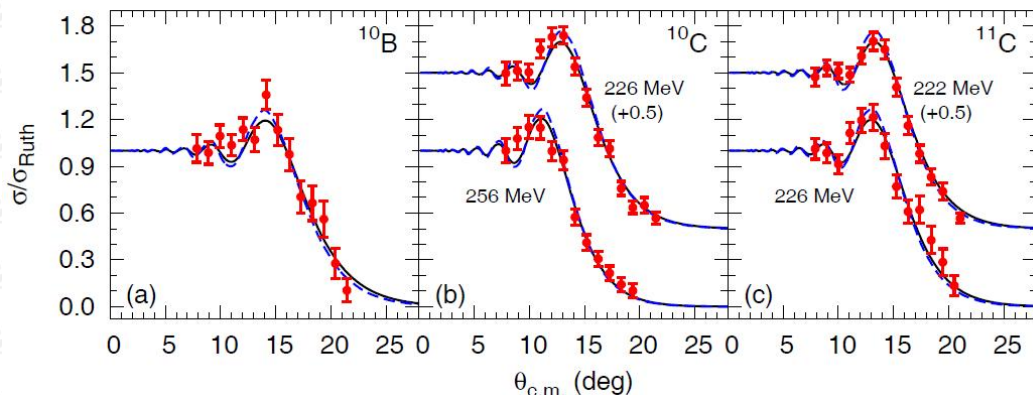
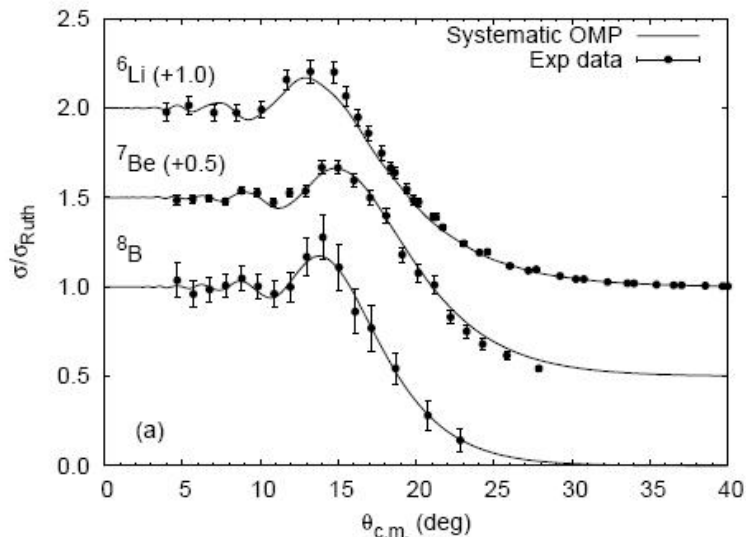
$Y(\theta)_{\text{Exp}}$, $Y(\theta)_{\text{Sim}}$ are the counts at a given angle θ from the experiment and the simulation, respectively.

Y.Y.Yang, J.S.Wang et al. NIMA701(2013)1



Y.Y.Yang, J.S.Wang et al. NIMA701(2013)1

轻质量奇特核的弹性散射研究



- 研究并提出了弹性散射1/4角的规律。
- 提出了描述不同核反应系统在低能区的核反应总截面的唯像公式
- 发展了在RIBLL上精确测量不稳定核弹性散射的实验方法。
- 发现质子滴线核 ${}^8\text{B}$ 、 ${}^9\text{C}$ 与重靶弹性散射中没有库仑核势干涉峰的削弱现象。

- Phys.Rev.C86 (2012)057602
- Phys.Rev.C86 (2012)057603
- Phys.Rev.C87 (2013)044613
- Phys.Rev.C90 (2014)014606
- Nucl.Inst.Meth.Phys.Res.A701(2013)1-6
- Phys.Rev.C94 (2016)034614

^8B 弹性的破裂反应截面

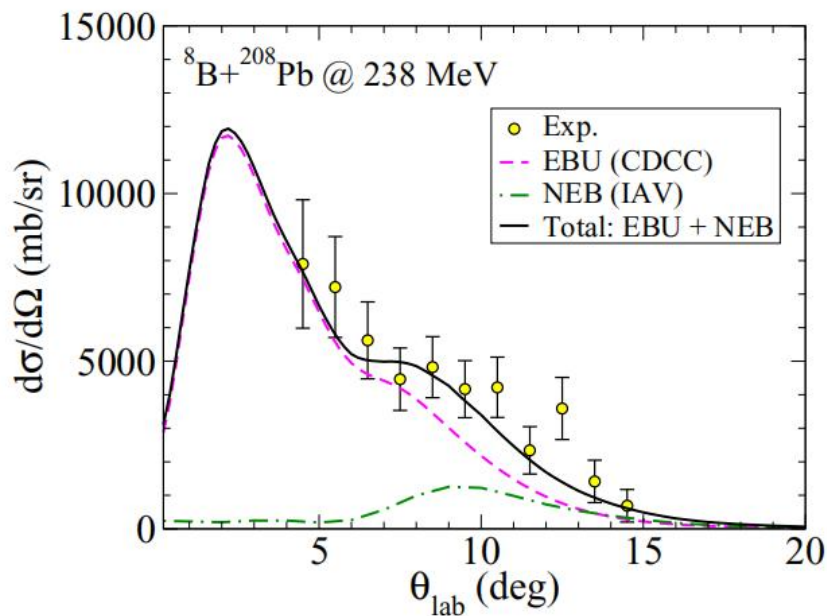
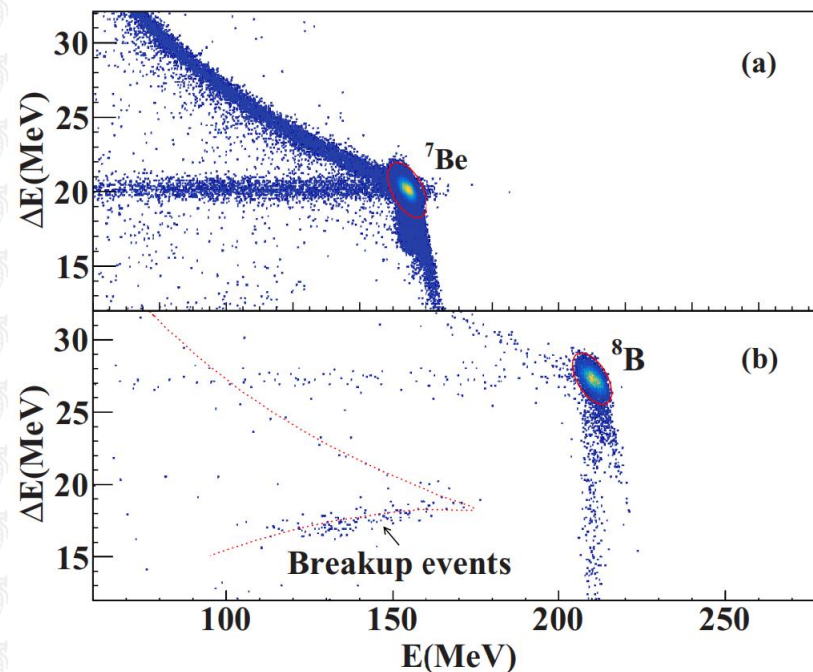
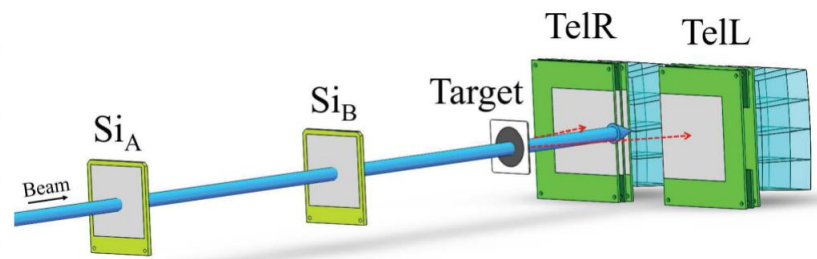
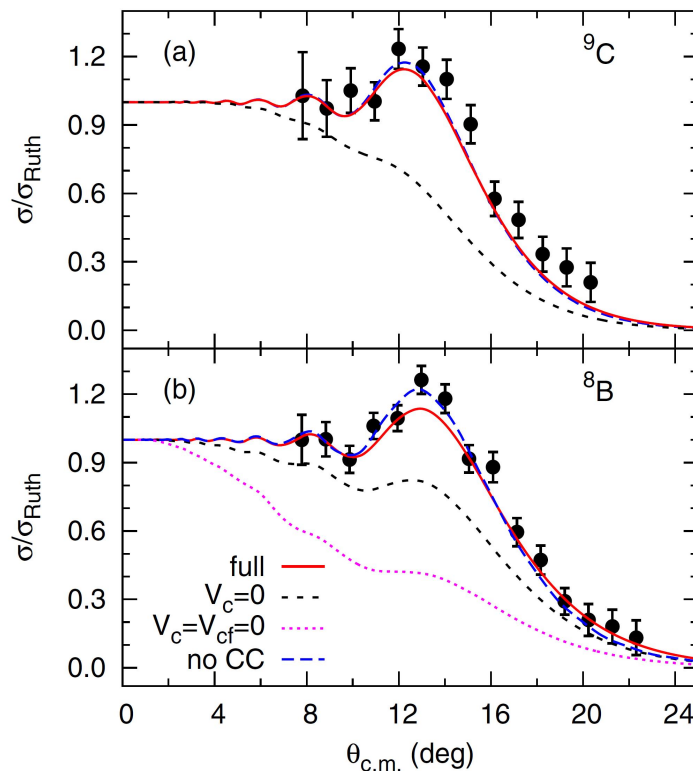
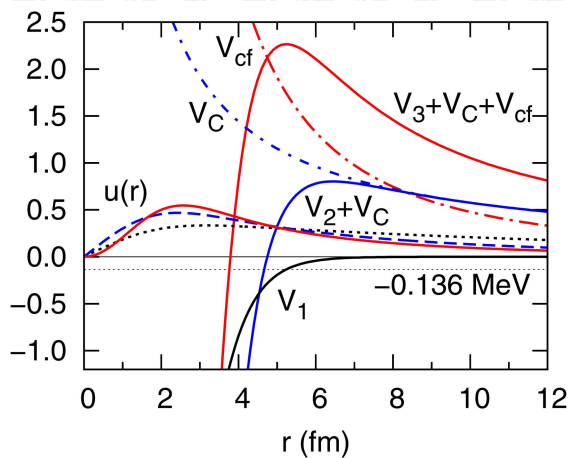
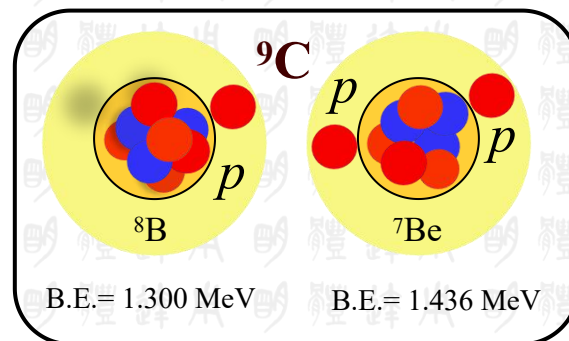
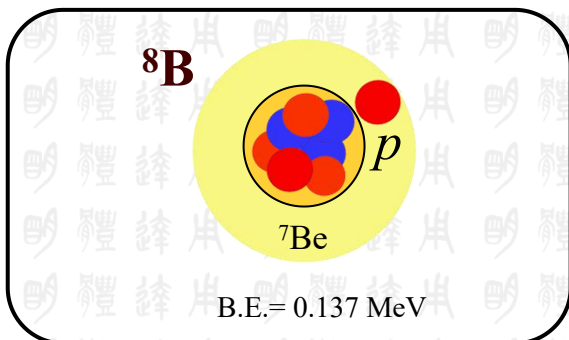


FIG. 5. Experimental ^7Be angular distributions from the $^8\text{B} + ^{208}\text{Pb}$ reaction at $E_{\text{lab}} = 238$ MeV (yellow circle) and comparisons with calculations. Error bars are statistical only.



K. Wang, Y.Y. Yang, ... JW, ... PRC 103, 024606 (2021)



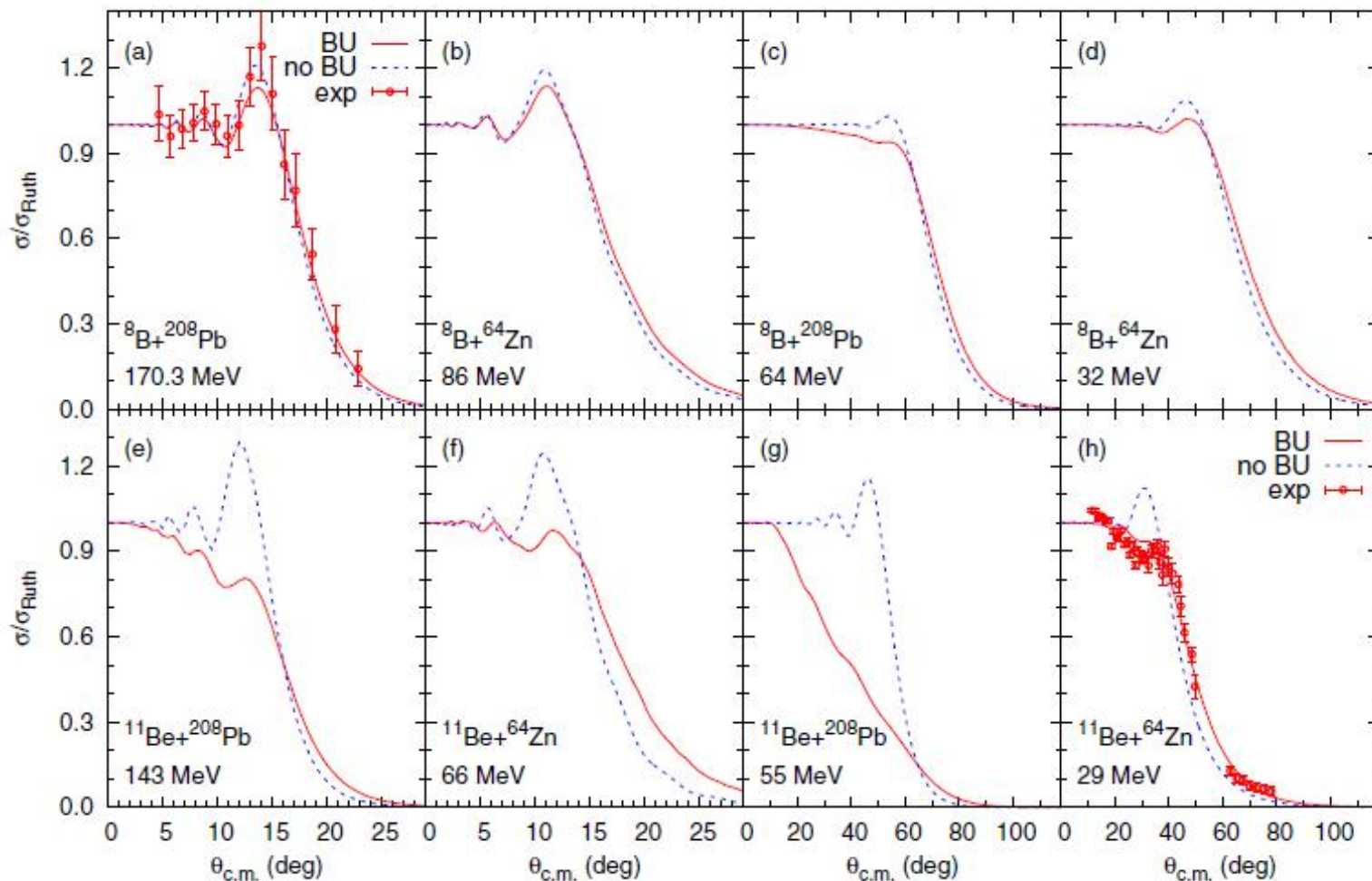
The problem is that the experiment has been done at energies where one should not expect a suppression of the Fresnel peak. I do not think one can extract conclusions about possible halo effects of ${}^9\text{C}$ by measuring its elastic scattering on lead at these relatively high energies. The authors made a few statements in the abstract that I do not think are correct.

..... the promising halo candidate ${}^9\text{C}$ shows a negligible suppression of the Coulomb rainbow at these energies, similar to that of ${}^8\text{B}$.

Y.Y. Yang, ..., *JW*, ..., PRC 98, 044608 (2018)



Breakup effects in ^8B and ^{11}Be : CCDC Calculations



Y. Y. Yang, X. Liu, D. Y. Pang, Phys. Rev. C (2016) 94, 034614

3.5倍库仑位垒的 ^{11}Be 弹性散射

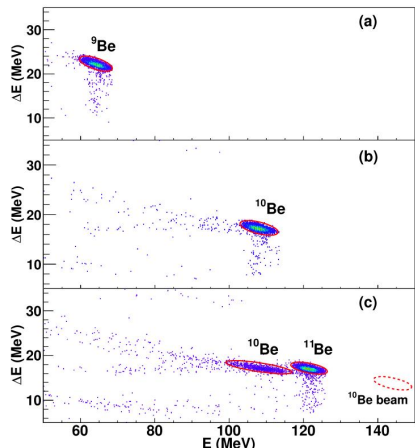


Fig. 2. The two-dimensional $\Delta E - E$ particle identification spectra for the (a) ^9Be , (b) ^{10}Be and (c) ^{11}Be beams within all the angles covered by the current measurement. In (c), the expected loci of ^{10}Be beam contamination are indicated and it is well separated from the group of ^{10}Be breakup fragment particles.

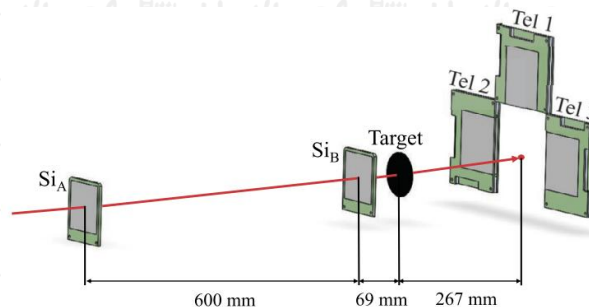


Fig. 1. Schematic view of the experimental setup.

F.F.Duan, Y. Y. Yang, ..., JW et al., PhysLettB.811.135942

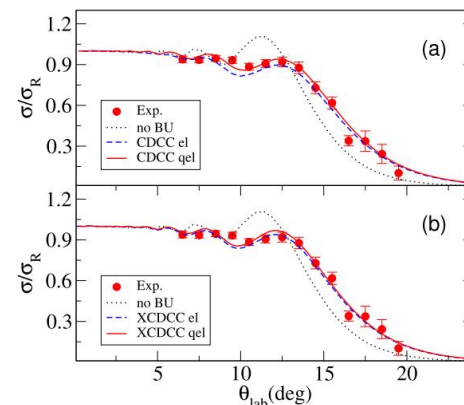


Fig. 4. Comparisons between results of CDCC (upper panel) and XCDCC (lower panel) calculations and the experimental data of the quasielastic scattering of $^{11}\text{Be} + ^{208}\text{Pb}$ at $E_{\text{lab}} = 140$ MeV. The dashed and dotted curves are for elastic scattering with and without including the continuum-continuum couplings, respectively. The solid curves are for quasielastic scattering, which are sums of elastic and inelastic scattering.

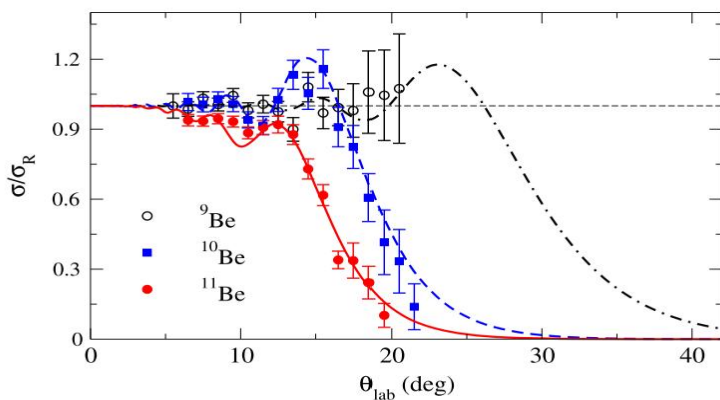


Fig. 3. Quasielastic scattering angular distributions for $^9,^{10},^{11}\text{Be} + ^{208}\text{Pb}$. The dash-dotted, dashed and solid curves are results of optical model calculations for ^9Be , ^{10}Be , and ^{11}Be , respectively. See the text for details.

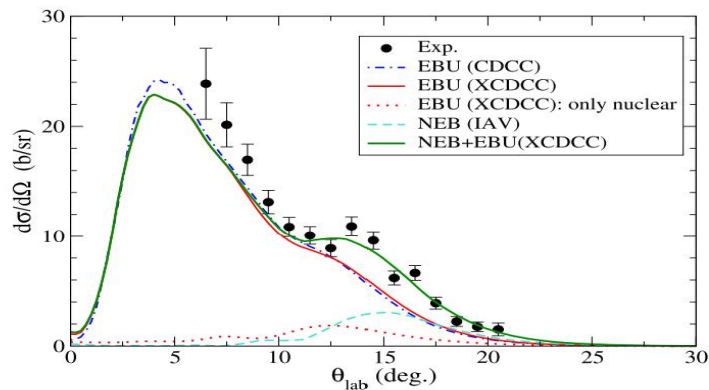


Fig. 5. Experimental differential breakup cross section for $^{11}\text{Be} + ^{208}\text{Pb}$ system at $E_{\text{lab}} = 140$ MeV compared with the CDCC and XCDCC calculations, for the elastic breakup part, and IAV calculations, for the NEB part. See text for the details.

5.2倍库伦位垒的 ^{11}Be 弹散数据

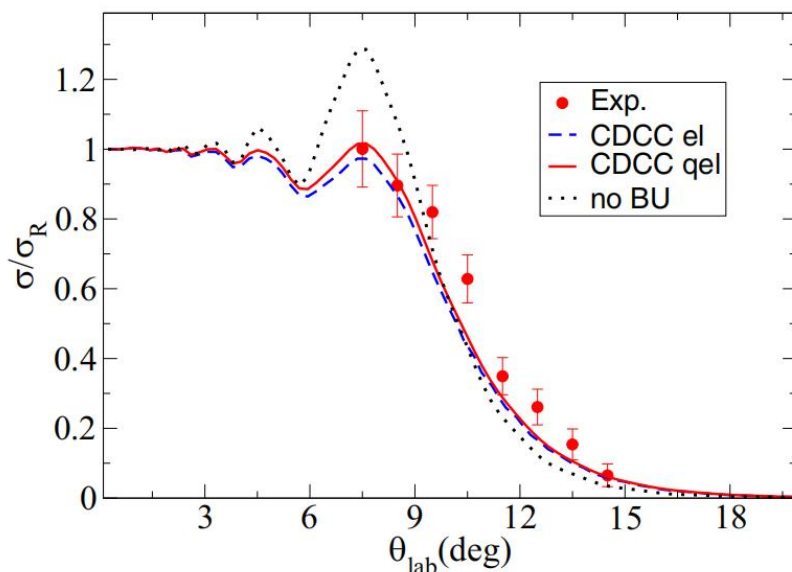


FIG. 3. The results of CDCC calculations and the experimental data of the quasielastic scattering of $^{11}\text{Be} + ^{208}\text{Pb}$ at $E_{\text{lab}} = 210$ MeV. The blue dashed, red solid, and black dotted curves are results of CDCC calculations of elastic and quasielastic scatterings and of no-continuum states, respectively.

F. F. Duan, Y.Y. Yang, ... JW et al., Phys. Rev. C
105, 034602 (2022)

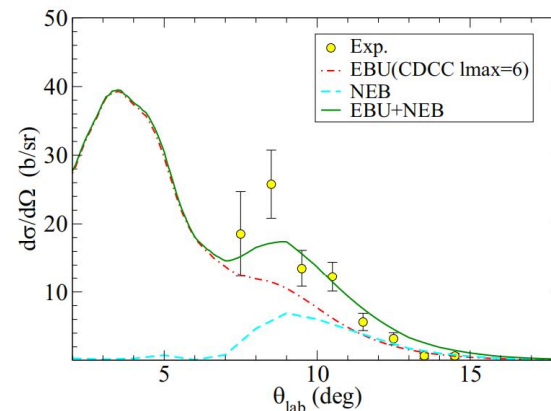


FIG. 6. Experimental breakup differential cross section, as a function of the ^{10}Be laboratory scattering angle, for the $^{11}\text{Be} + ^{208}\text{Pb}$ system at $E_{\text{lab}} = 210$ MeV compared with the calculations. See text for the details.

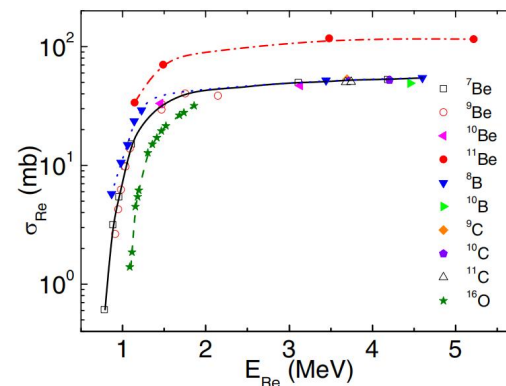
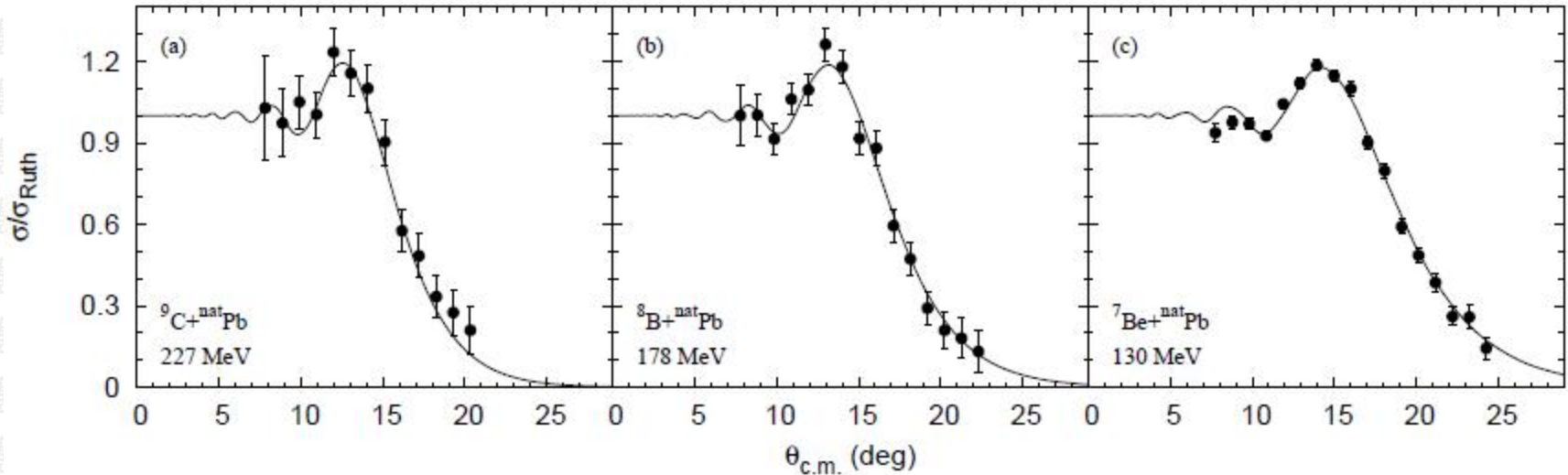


FIG. 7. Reduced reaction cross sections for several projectiles on several medium- to heavy-mass targets. The curves are to guide the eye.

Elastic scattering of Proton Drip Line Nuclei

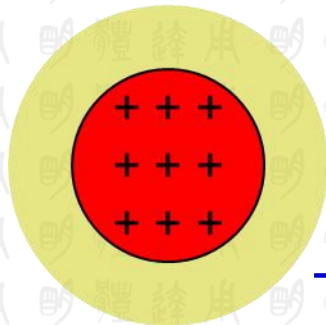
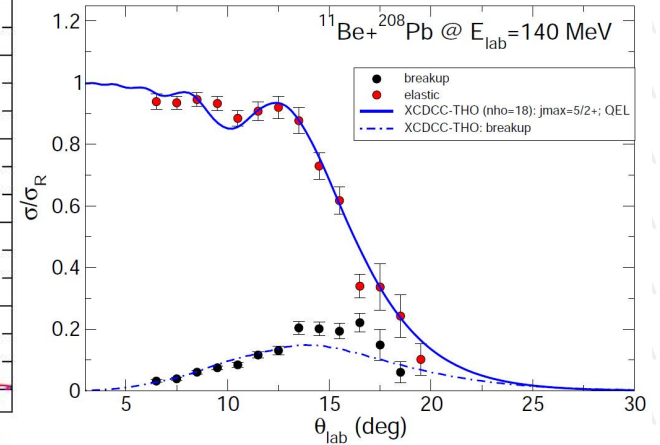
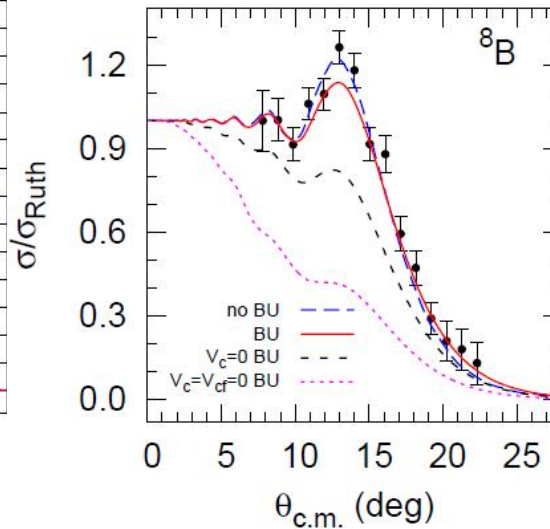
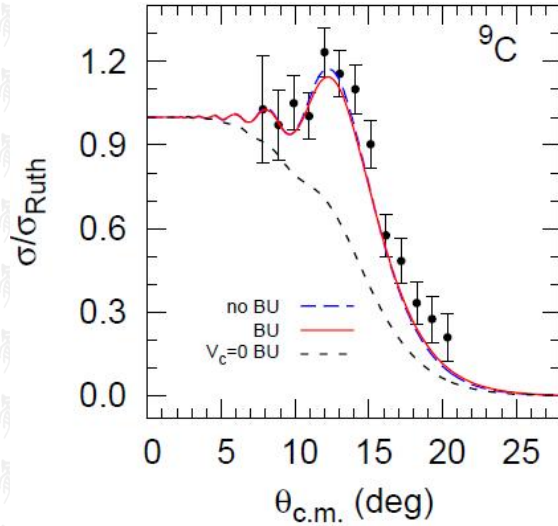


The experimental data can be reproduced by the optical model calculations with the systematic nucleus-nucleus potential of Xu and Pang.

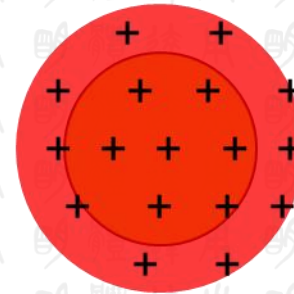
Yanyun Yang, ..., JW et al. PRC98 (2018) 044608



Why the Coulomb rainbow peak not suppressed for proton-rich nuclei ?



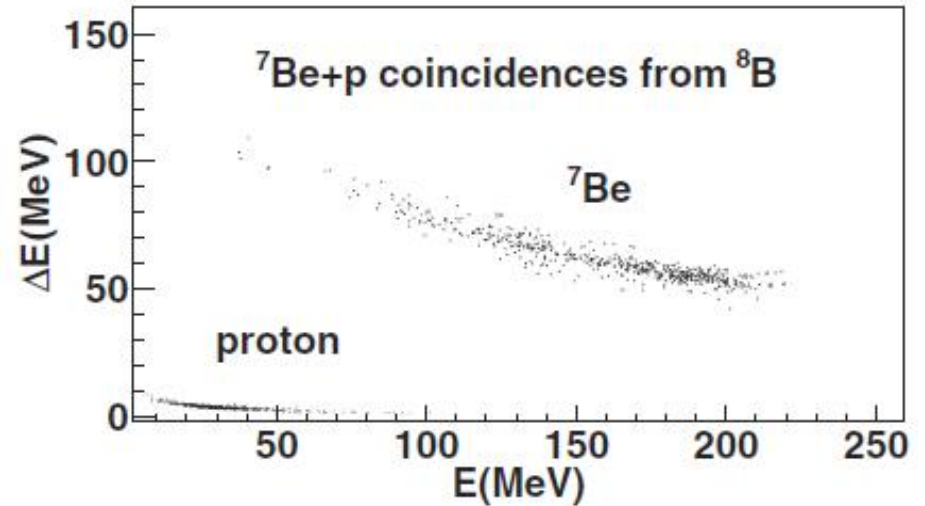
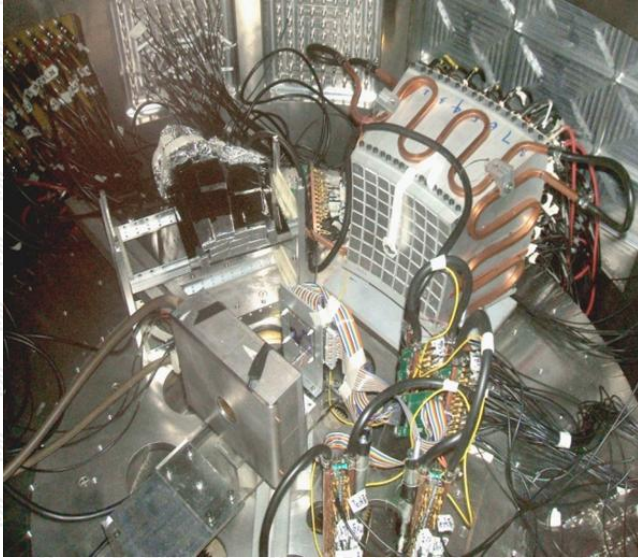
NO proton halo?



The different structure between proton and neutron halo

${}^8\text{B}$ 的破裂反应机研究

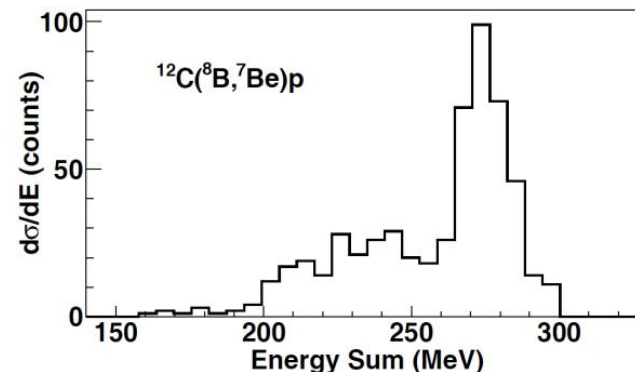
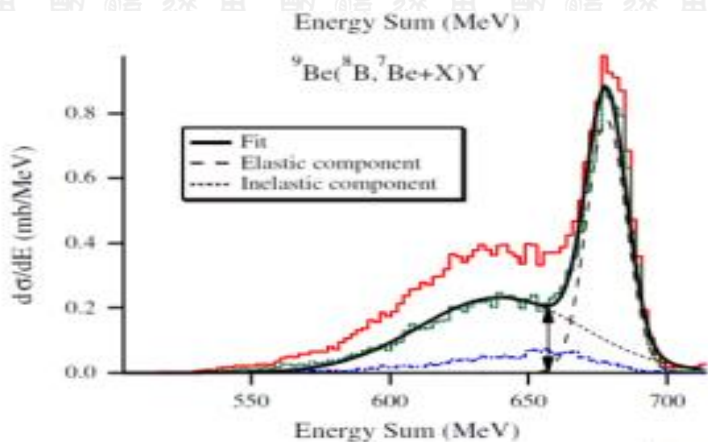
Experimental Setup



$^{12}\text{C}(^8\text{B}, ^7\text{Be})\text{p}$ @36.7MeV/u

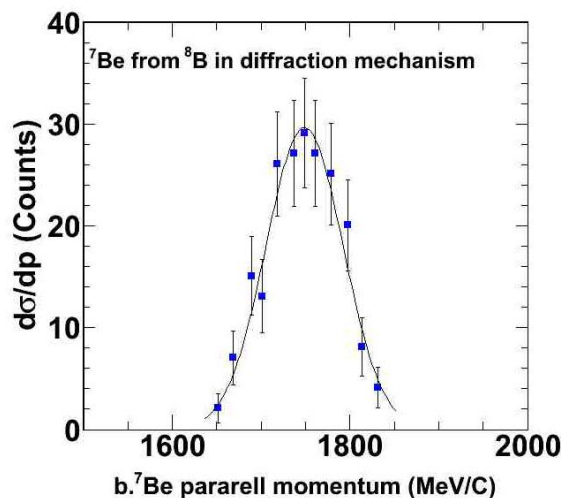
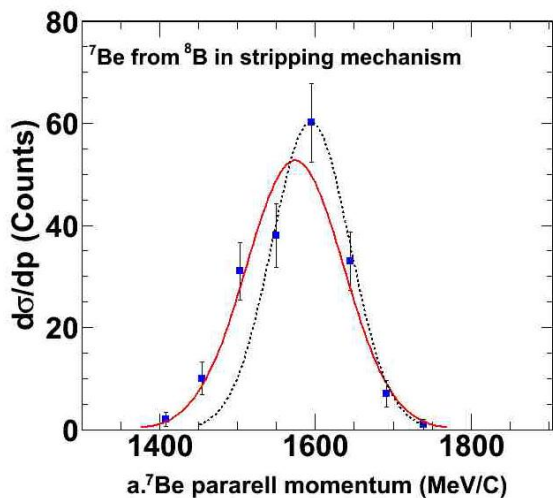


Identifying the reaction mechanism



MSU $^8\text{B}@86.7\text{MeV}$ D.Bazin et al., PRL 102,232501

Present work



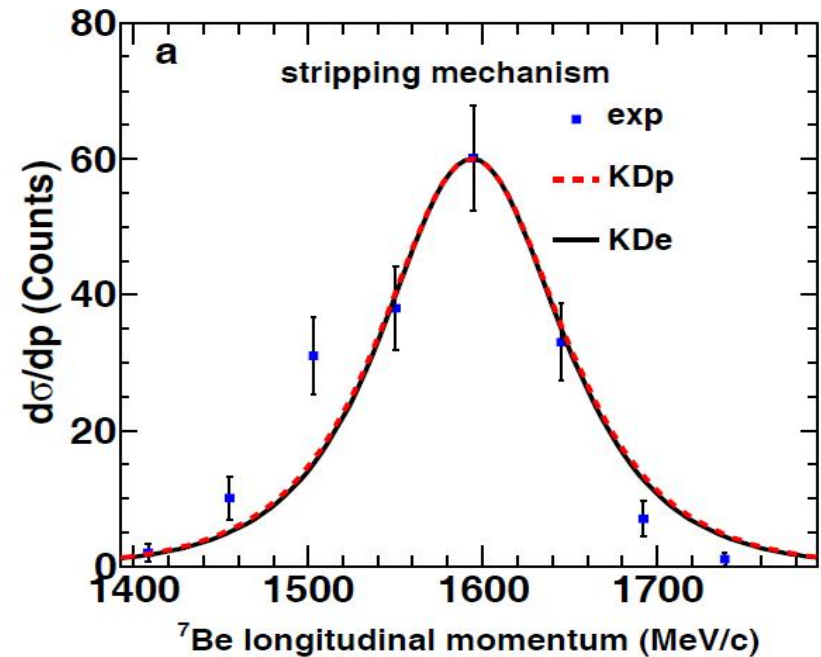
Width by fitting:
 Diffractive:
 $92 \pm 7\text{MeV/c}$
 Stripping:
 $124 \pm 17\text{MeV/c}$

Theoretical Calculations-Stripping

The stripping momentum distributions were calculated using the **eikonal approximation formalism** (PRC70, 034609) and the eikonal phase shifts and S-matrices of the following potentials (denoted KDe)

The complex ${}^7\text{Be}$ -target optical potential was calculated using the double-folding method of PRC74,064604, assuming Gaussian ${}^7\text{Be}$ and ${}^{12}\text{C}$ densities of rms radii 2.31 and 2.32 fm. The proton-target potential was calculated from the Koning and Delaroche global parameterization (NPA713, 231)

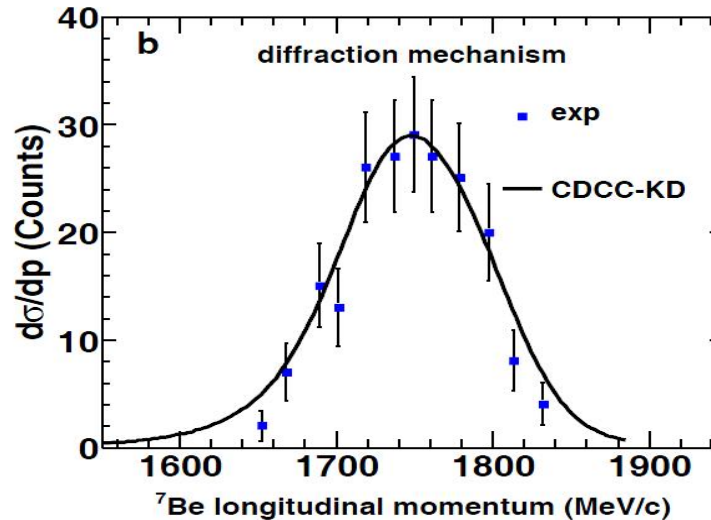
In addition, due to the relatively low beam energy, calculations were repeated using the improved description of the proton-target S-matrix (denoted KDp).



The ${}^8\text{B}(\text{g.s.})$ to ${}^7\text{Be}$ final state radial overlaps and spectroscopic factors were taken from PRL102,232501

Calculation done by Prof. J. A. Tostevin

Theoretical Calculations-Diffraction



The diffraction mechanism differential cross sections were calculated using a CDCC (Coupled Discretized Continuum Channels) breakup model space as PRL102,232501, and the resulting momentum distributions constructed by integration over the solid angles covered by the current detection system, as is discussed in Phys. Rev. C **66**, 024607.

Calculation done by Prof. J. A. Tostevin

A summary of width calculated in different model

Summary of the distributions measured in this work and calculated in different model

	<i>present work</i>	CDCC	KDe	KDp	Hencken	Hensen	Esbensen
	(MeV/c)	(MeV/c)	(MeV/c)	(MeV/c)	(MeV/c)	(MeV/c)	(MeV/c)
Stripping	124(17)		103	107	151	153/75	166/82
Diffraction	92(7)	101			93		

85 ± 4 ^{8}B @41AMeV PRL77(1996)5020

The experimental data show the width of longitudinal momentum distribution for stripping breakup is obviously wider than diffraction breakup.

S.L.Jin, J.S.Wang et al., Phys. Rev. C91,054617(2015)



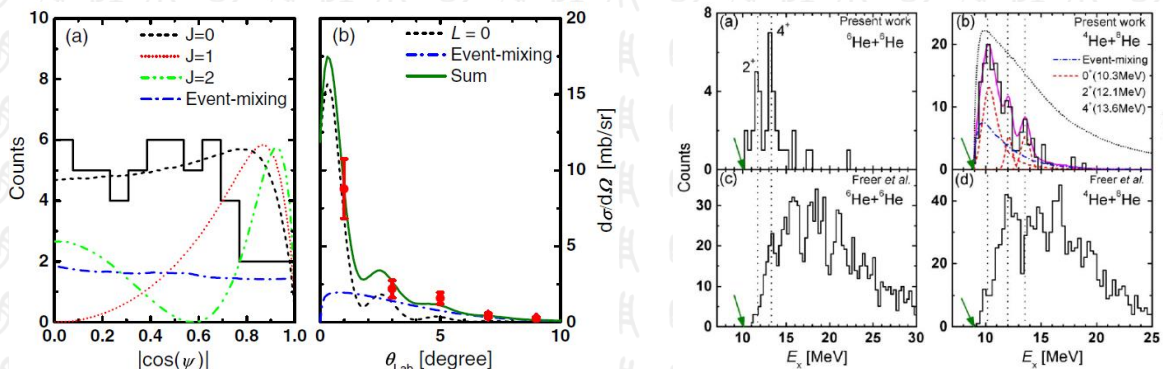
PHYSICAL REVIEW C 91, 054617 (2015)

Reaction mechanism of ^8B breakup at the Fermi energy

S. L. Jin (金仕纶),^{1,2} J. S. Wang (王建松),^{1,*} Y. Y. Yang (杨彦云),¹ P. Ma (马朋),¹ M. R. Huang (黄美容),¹
J. B. Ma (马军兵),¹ F. Fu (付芬),¹ Q. Wang (王琦),¹ M. Wang (王猛),¹ Z. Y. Sun (孙志宇),¹ Z. G. Hu (胡正国),¹
R. F. Chen (陈若富),¹ X. Y. Zhang (张雪茛),¹ X. H. Yuan (袁小华),¹ X. L. Tu (涂小林),¹ Z. G. Xu (徐志国),¹ K. Yue (岳珂),¹
J. D. Chen (陈金达),¹ B. Tang (唐彬),¹ Y. D. Zang (臧永东),¹ D. P. Wu (武大鹏),¹ Q. Hu (胡强),¹ Z. Bai (白真),¹
Y. J. Zhou (周远杰),^{1,2} W. H. Ma (马维虎),^{1,2} J. Chen (陈杰),^{1,2} C. J. Lin (林承键),³ X. X. Xu (徐新星),³ Z. Z. Ren (任中洲),⁴
C. Xu (许昌),⁴ D. D. Ni (倪冬冬),⁴ Y. H. Zhang (张玉虎),¹ H. S. Xu (徐珊瑚),¹ and G. Q. Xiao (肖国青)¹

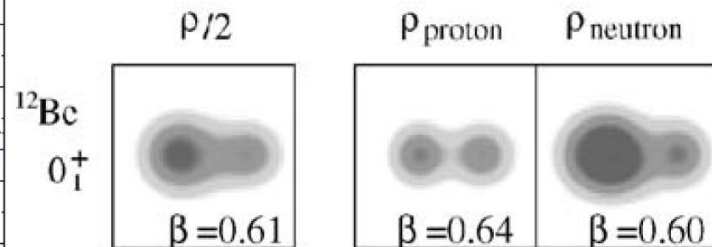
原子核的3核子 (t 、 ${}^3\text{He}$) 集团 和纯中子集团

^{12}Be 的团簇结构研究

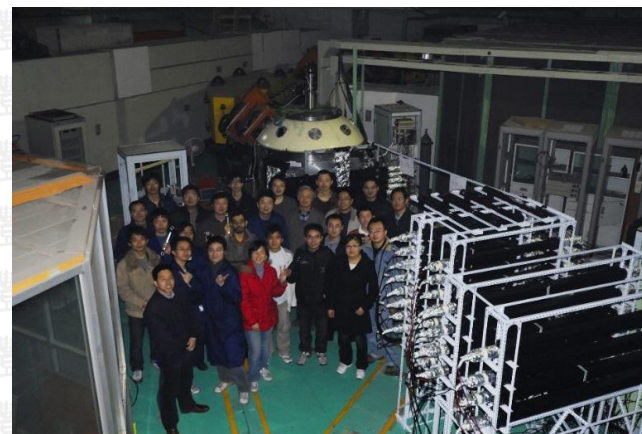


Phys. Rev. Lett. 112(2014) 162501
Phys. Rev. C 91 (2015) 024304

- **First observation of enhanced monopole transition in ^{12}Be** at excitation energy of 10.3 MeV, evidence for the existence of $^4\text{He}+^8\text{He}$ molecular rotation, an intensely investigated topic in the past decade
- **A new technique** of measurement at zero degree is developed to study the molecular states in exotic nuclei



Kanada en'yo et al., AMD calculations

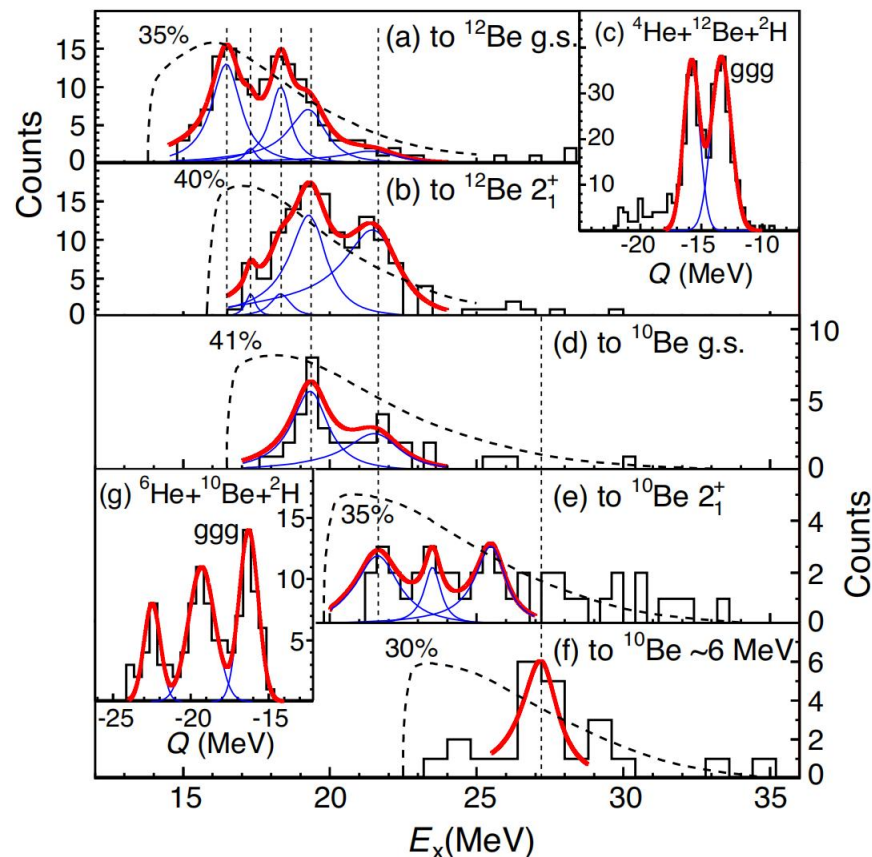
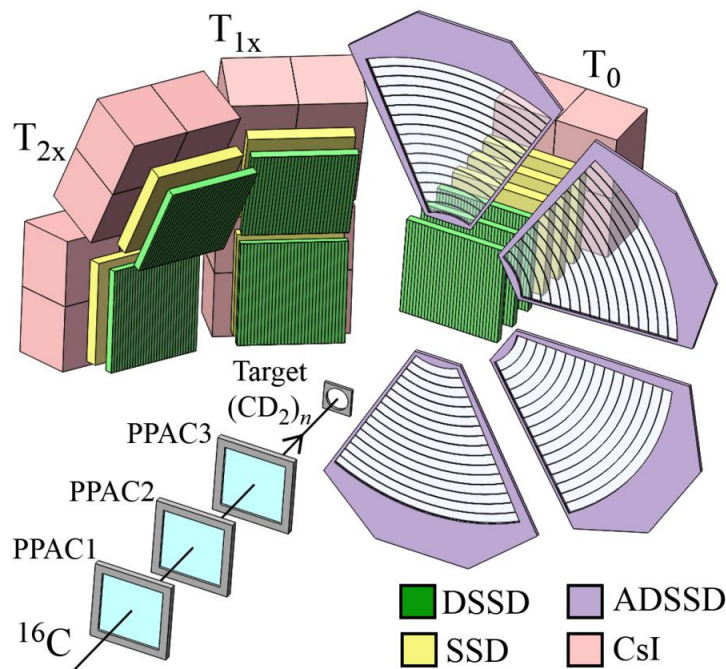


^{16}C 的链状分子结构

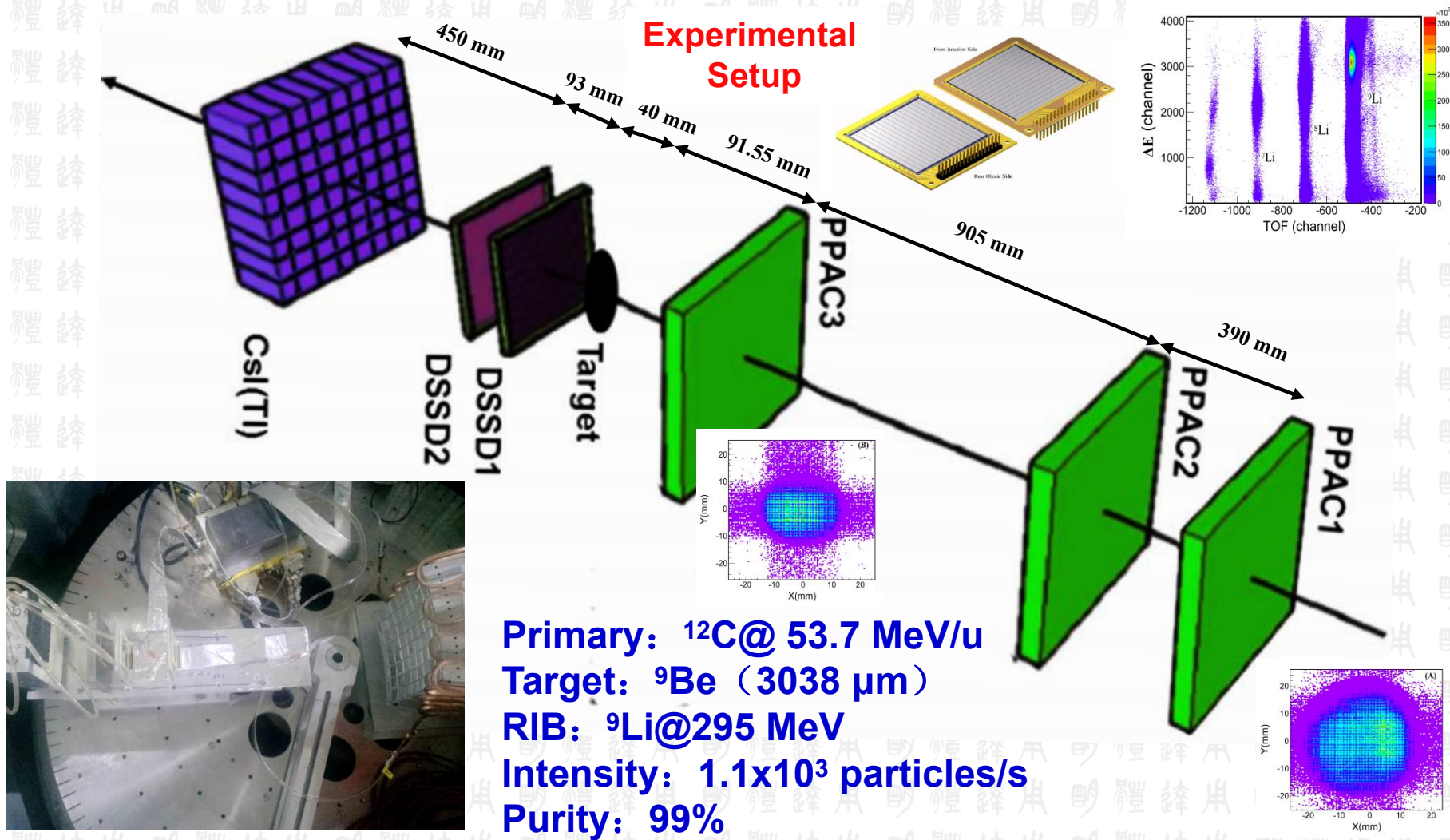
PHYSICAL REVIEW LETTERS **124**, 192501 (2020)

Positive-Parity Linear-C

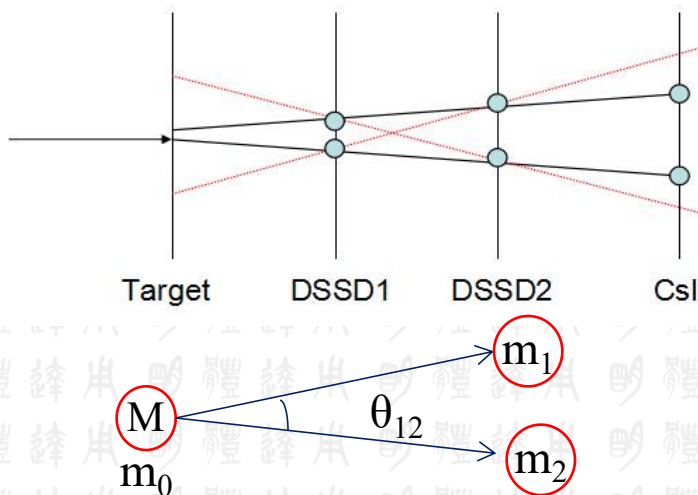
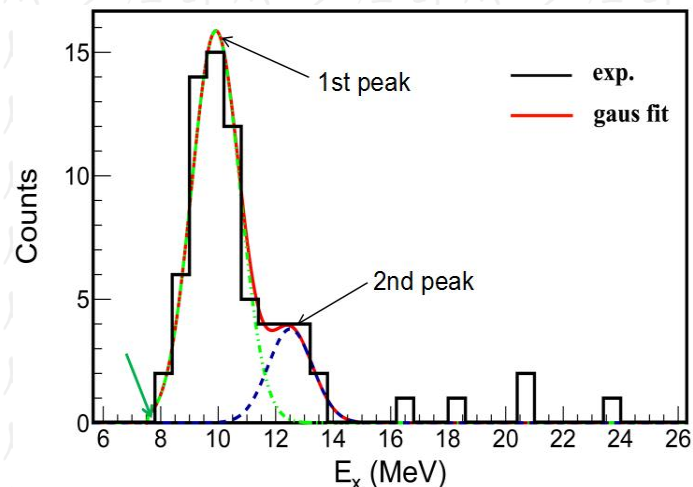
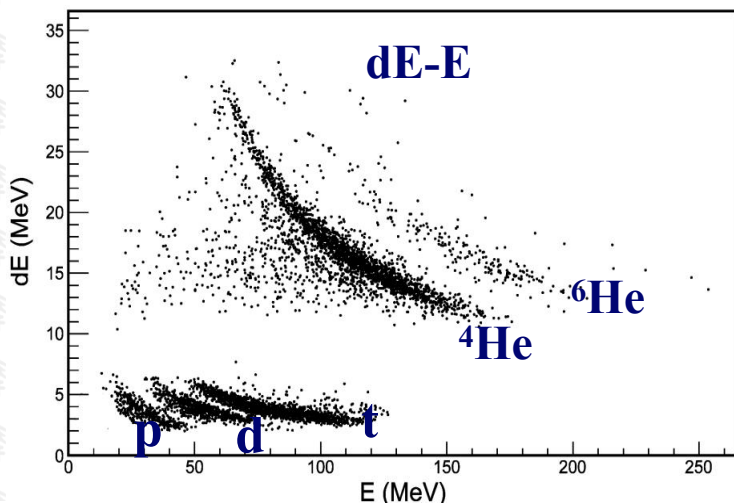
Y. Liu,¹ Y. L. Ye^{1,*}, J. L. Lou,¹ X. F. Yang¹, T. Baba,² J. H. Han,³ H. Hua,¹ J. S. Wang,^{4,5} Y. Y. Yang,⁵ P. Ma,⁵ Z. Bai,⁵ Q. Hu,¹ J. Feng,¹ H. Y. Wu,¹ J. X. Han,¹ S. W. Bai,¹ G. Li,¹ H. Z. Yang,¹



Experimental Setup



Event Selection and Reconstruction



Invariant mass:

$$M = \sqrt{(E_1 + E_2)^2 - [|\mathbf{P}_1|^2 + |\mathbf{P}_2|^2 + 2|\mathbf{P}_1||\mathbf{P}_2|\cos(\theta_{12})]};$$

$$E_i = T_i + m_i; \quad |\mathbf{P}_i|^2 = T_i^2 + 2T_i m_i; \quad \theta_{12} = \langle \mathbf{P}_1, \mathbf{P}_2 \rangle;$$

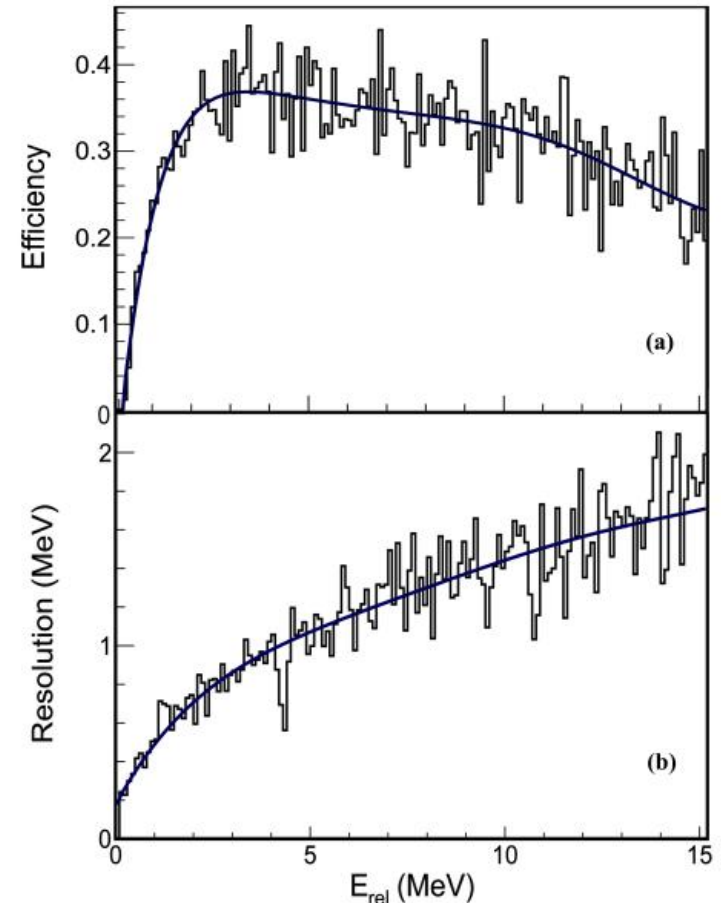
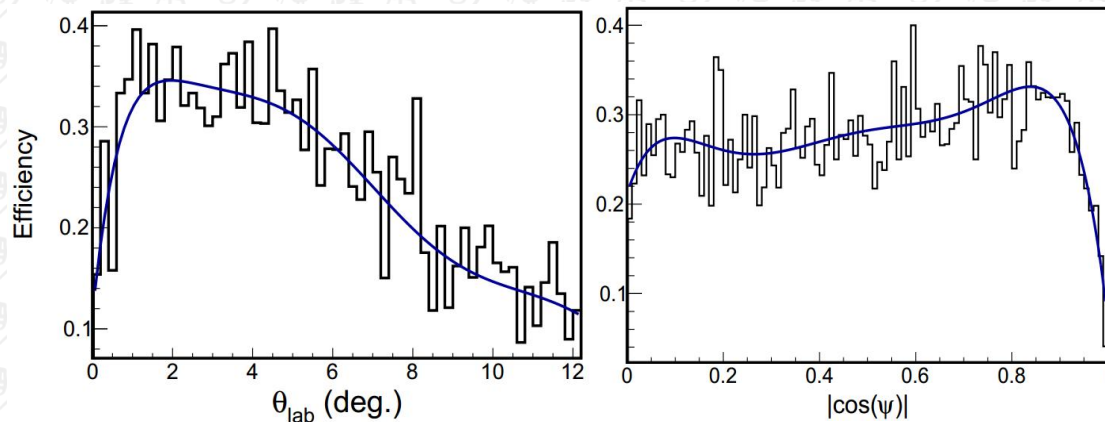
Excitation energy: $E_x = M - m_0$

Relative energy: $E_{rel} = E_x - E_{thr}$

Threshold energy of ${}^6\text{He}+t$: $E_{thr} = 7.588 \text{ MeV}$

Simulation of Detector efficiency

A Monte Carlo simulation is performed to determine the detection efficiency according to the geometry, assuming isotropic emission of the fragments in the center of mass frame.

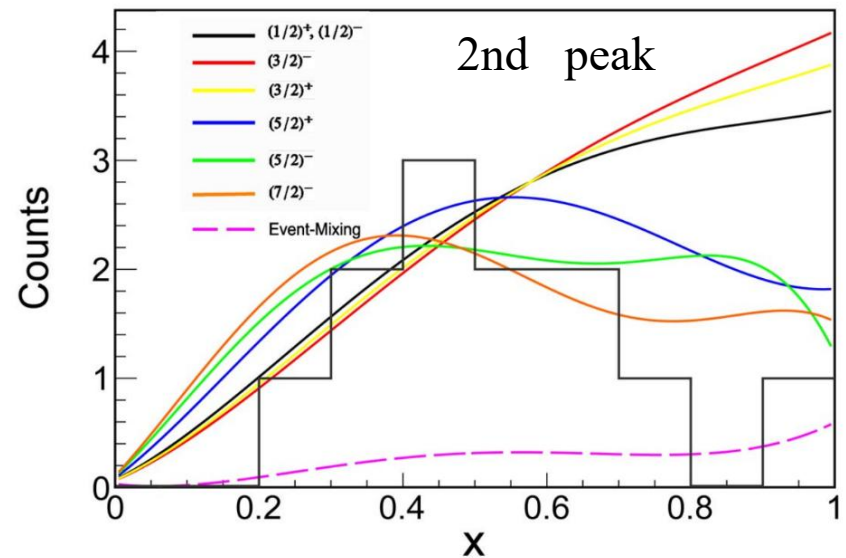
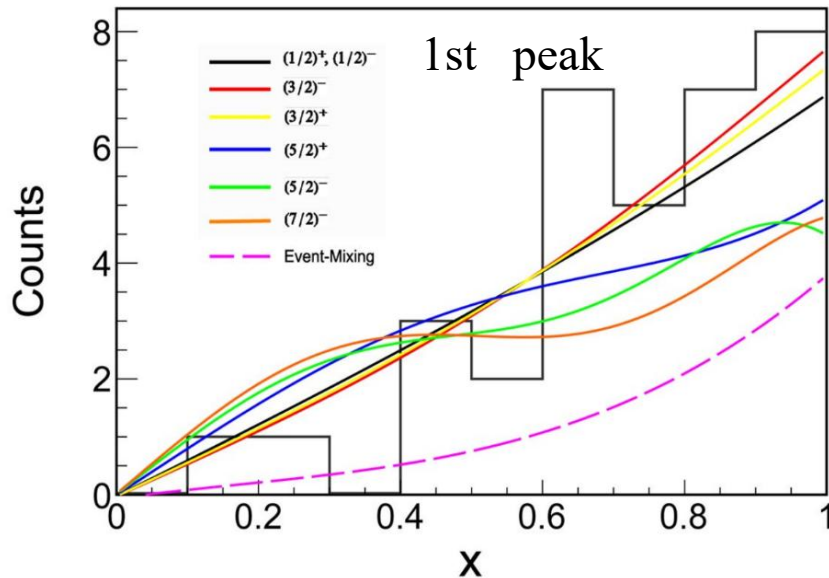
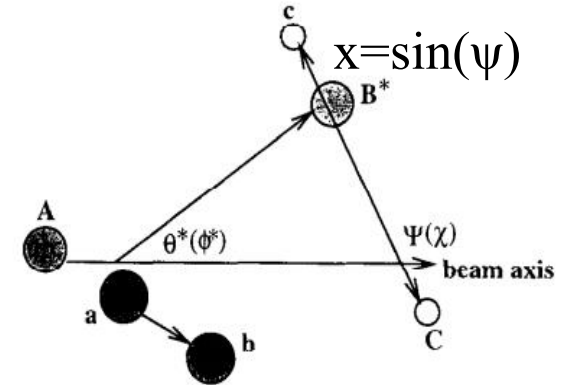


Angular Correlation Analysis

G. Finkel et al., Phys. Rev. C19 (1979) 1782

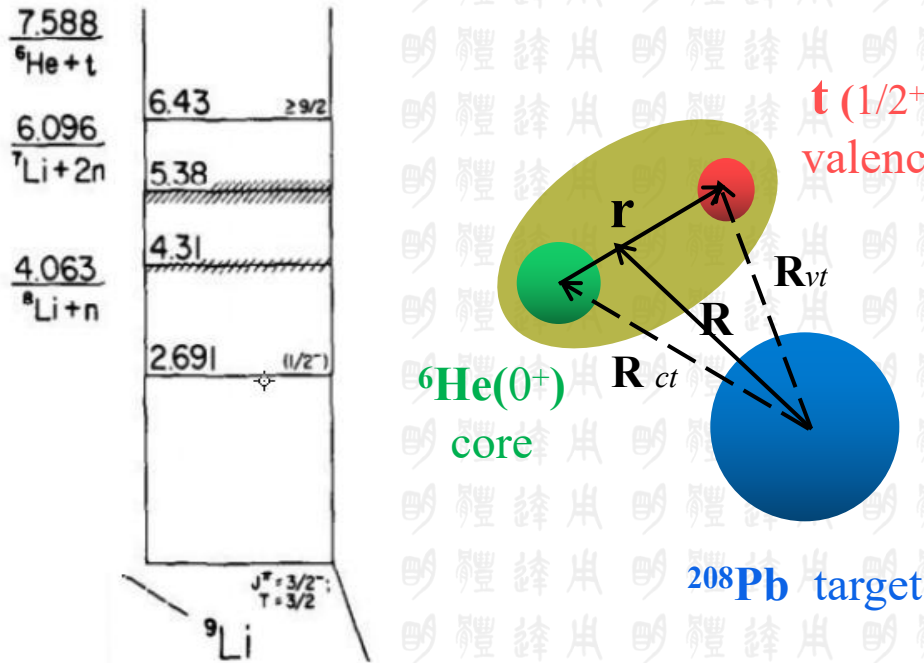
$$N(\Omega^*, \Omega_\psi) \propto \sum_{m_{Li} = -\frac{3}{2}}^{\frac{3}{2}} \sum_{m_t = -\frac{1}{2}}^{\frac{1}{2}} \left| \sum_{m_{Li^*}} T_{m_{Li^*}}^{m_{Li}} (L m_L S m_t | J_{Li^*} m_{Li^*}) Y_L^{m_L}(\psi, \chi) \right|^2$$

The relative momentums of the two clusters are determined to be 1 for the 1st peak and 2 for the 2nd peak respectively.

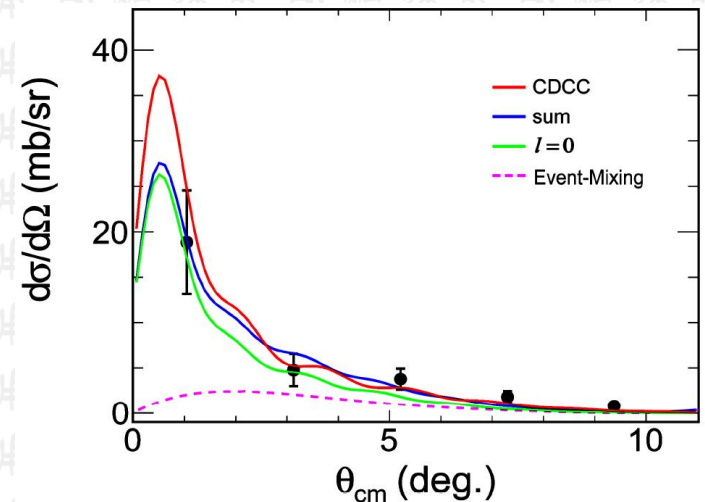
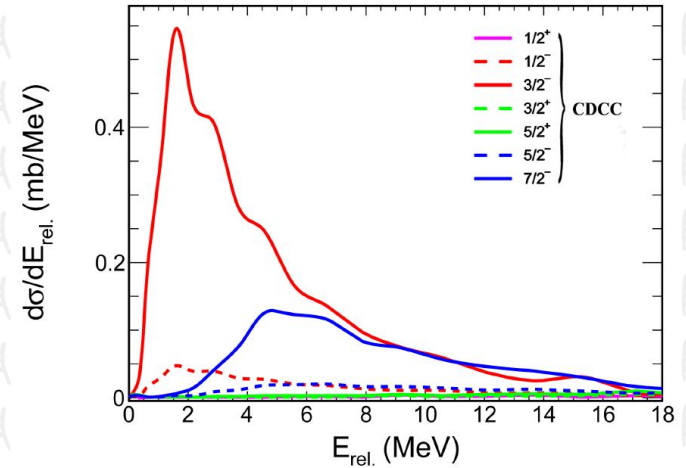


CDCC Analysis

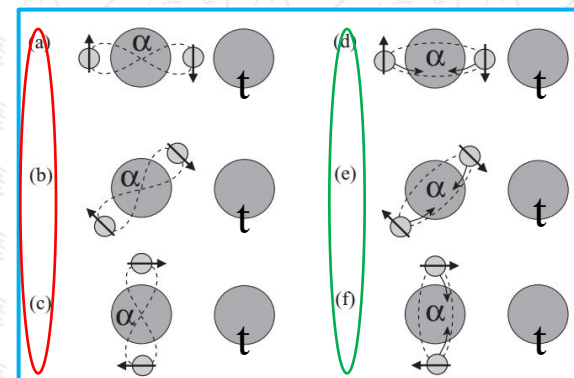
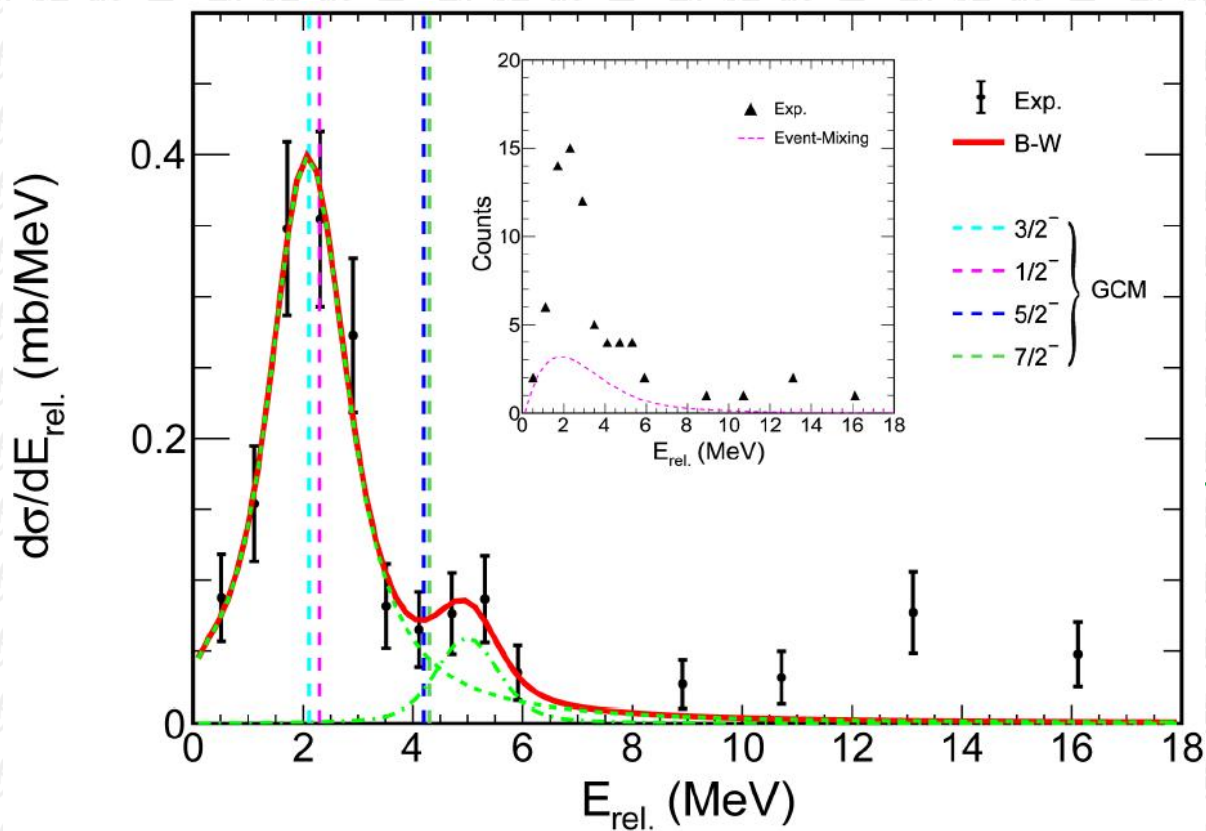
${}^9\text{Li}$ modeled as 2-body projectile



${}^9\text{Li}$ ground state $p3/2^-$



Comparison with GCM predictions



Y. Kanada-En'yo and T. Suhara, PRC 85, 024303(2012).

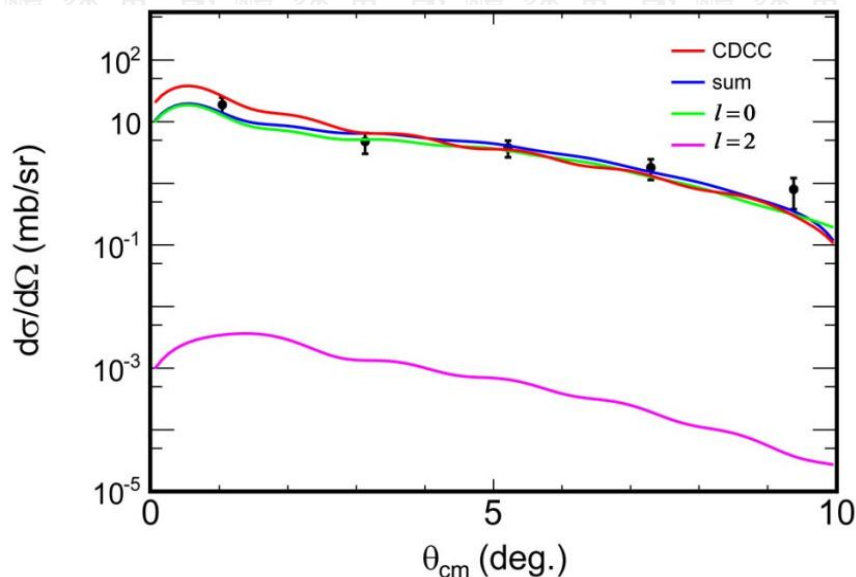
Yoshiko Kanada-En'yo, PRC 94, 024326 (2016).



Multipole-Decomposition Analysis

$$\left(\frac{d\sigma}{d\Omega}\right)_{\text{exp}} = \sum_l a_l \cdot \left(\frac{d\sigma}{d\Omega}\right)_{l,DWBA}$$

the DWBA cross sections exhausting the full EWSR for the transferred angular momentum l



Monopole transition potential:

$$G_0(r) = \alpha_0^U \left[3U(r) - r \frac{dU(r)}{dr} \right]$$

Quadrupole transition potential :

$$G_2(r) = -\delta_2^U \frac{dU(r)}{dr}$$

D. J. Horen et al. Phys Rev C 52(1995) 1554

B. Bonin et al., Nucl. Phys. A 430 (1984) 349-396

$a_0=0.023(4)$; $M(ISO)=5.0 \pm 0.5(\text{stat.}) \text{ fm}^2$; GCM: $\sim 6 \text{ fm}^2$; Systematic error: 14%

Kanada-En 'Yo Y. Phys.Rev.C 94 (2016) 024316.

Conclusions for $t+{}^6\text{He}$ cluster of ${}^9\text{Li}^*$

- Two resonant states are clearly observed with the excitation energies at 9.8 MeV and 12.6 MeV and spin-parity of $3/2^-$ and $7/2^-$ respectively by the method of angular correlation analysis and verified by the continuum discretized coupled channels (CDCC) calculation
- A monopole matrix element about 4 fm^2 for the $3/2^-$ state is extracted from the DWBA calculations
- These experimental results consist with the prediction of generator coordinate method (GCM), supporting the feature of clustering structure of two neutron-rich clusters in the ${}^9\text{Li}^*$

W. H. Ma et al., PhysRevC.103(2021)L061302

PHYSICAL REVIEW C **103**, L061302 (2021)

Letter

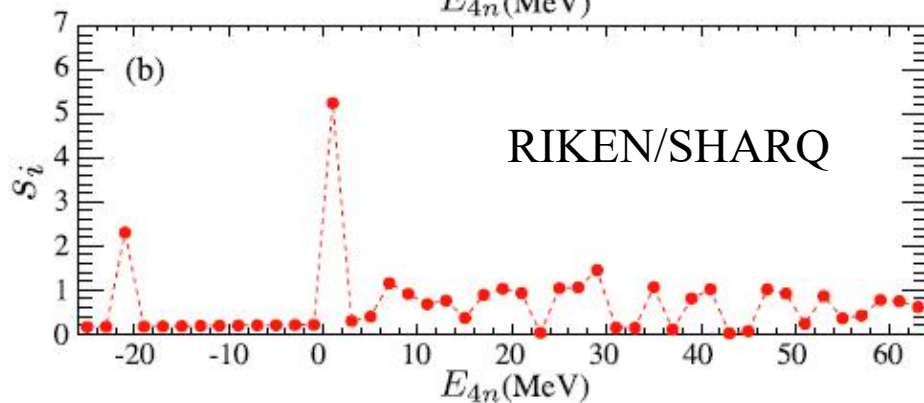
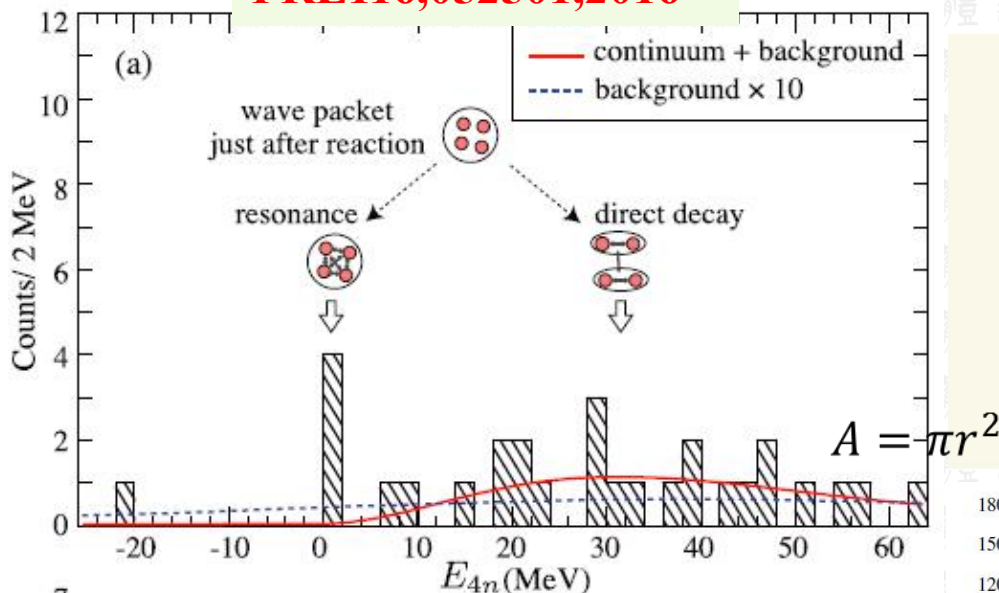
Observation of ${}^6\text{He} + t$ cluster states in ${}^9\text{Li}$

W. H. Ma (马维虎),^{1,2} D. Patel,^{1,3} Y. Y. Yang (杨彦云),¹ J. S. Wang (王建松) ,^{4,1,*} Y. Kanada-En'yo,⁵ R. F. Chen (陈若富),¹ J. Lubian ,⁶ Y. L. Ye (叶沿林),⁷ Z. H. Yang (杨再宏),⁷ Z. Z. Ren (任中洲),⁸ S. Mukherjee,⁹ J. B. Ma (马军兵),¹ S. L. Jin (金仕纶),¹ P. Ma (马朋),¹ J. X. Li (李加兴),¹⁰ Y. S. Song (宋玉收),¹¹ Q. Hu (胡强),¹ Z. Bai (白真),¹ M. R. Huang (黄美容),¹² X. Q. Liu (刘星泉),¹ Y. J. Zhou (周远杰),^{1,13} J. Chen (陈杰),^{1,13} Z. H. Gao (高志浩),¹ F. F. Duan (段芳芳),^{1,14} S. Y. Jin (金树亚),¹ S. W. Xu (许世伟),¹ G. M. Yu (余功明),¹ G. Z. Shi (石国柱),¹ Q. Wang (王琦),¹ T. F. Wang (王涛峰),¹⁵ X. Y. Ju (巨欣跃),¹⁶ Z. G. Hu (胡正国),¹ Y. H. Zhang (张玉虎),¹ X. H. Zhou (周小红),¹ H. S. Xu (徐瑚珊),¹ G. Q. Xiao (肖国青),¹ and W. L. Zhan (詹文龙)¹

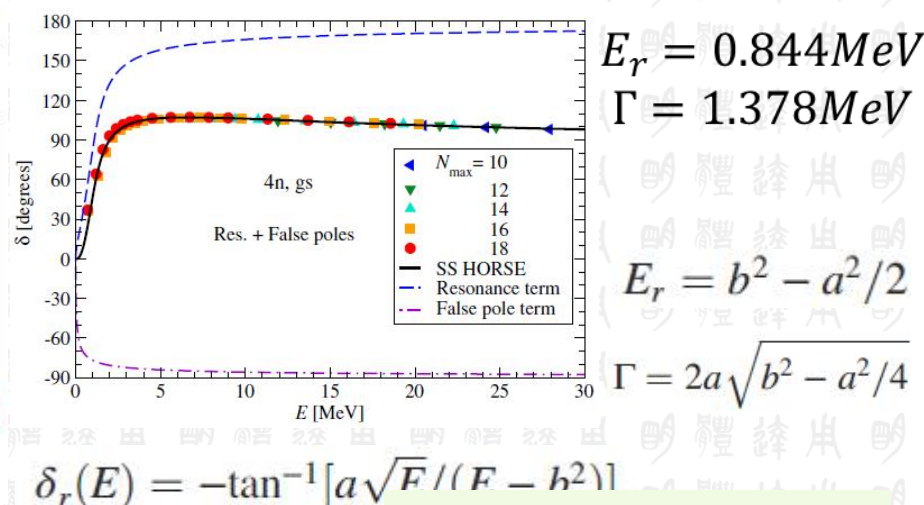
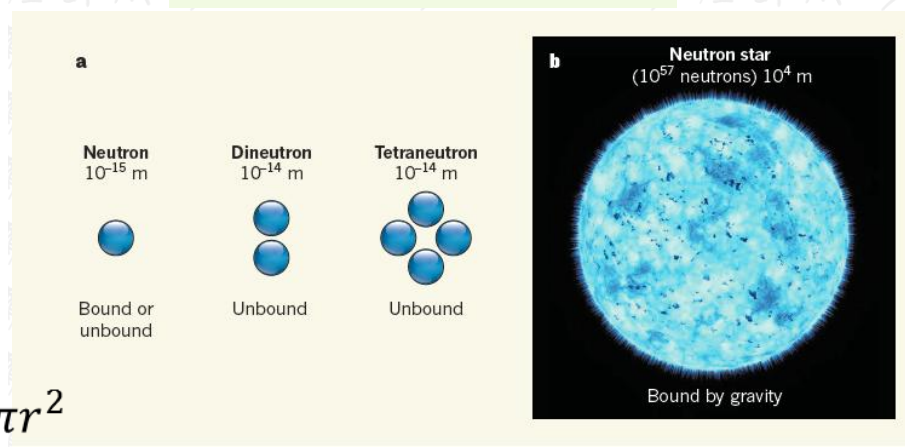
2016年热门话题: 4n 共振态

PRL116,052501,2016

Nature532.448(2016)



$$E_r = 0.83 \pm 0.65(\text{stat}) \pm 1.25(\text{syst}) \text{MeV}$$



$$E_r = 0.844 \text{MeV}$$

$$\Gamma = 1.378 \text{MeV}$$

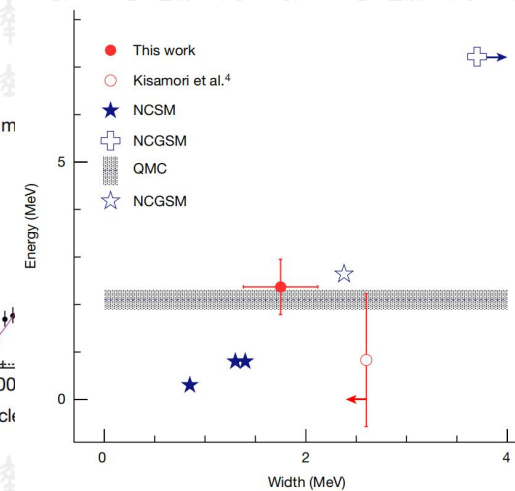
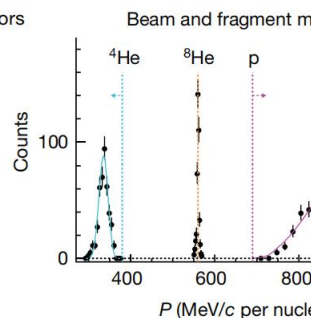
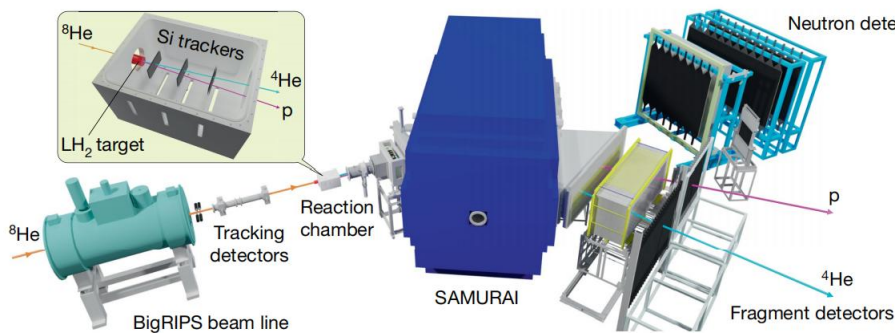
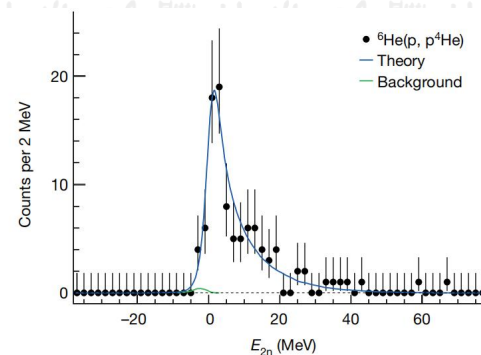
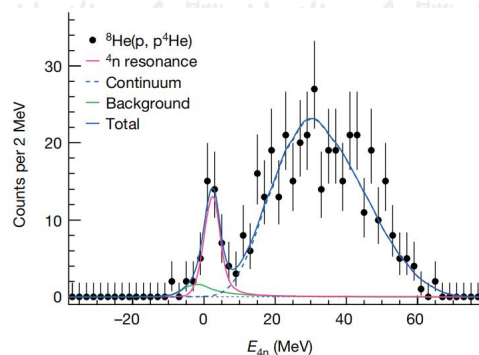
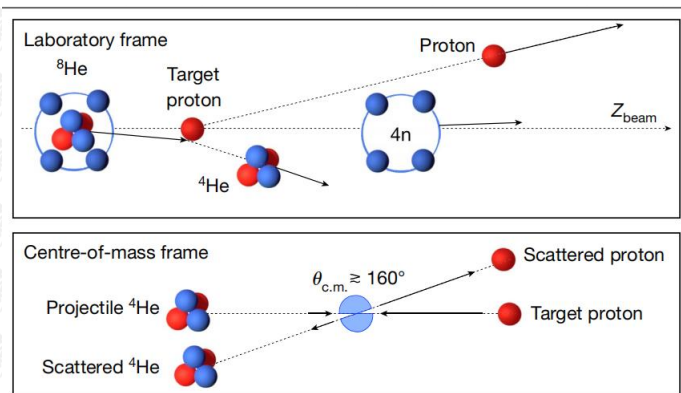
$$E_r = b^2 - a^2/2$$

$$\Gamma = 2a\sqrt{b^2 - a^2/4}$$

$$\delta_r(E) = -\tan^{-1}[a\sqrt{E}/(E - b^2)]$$

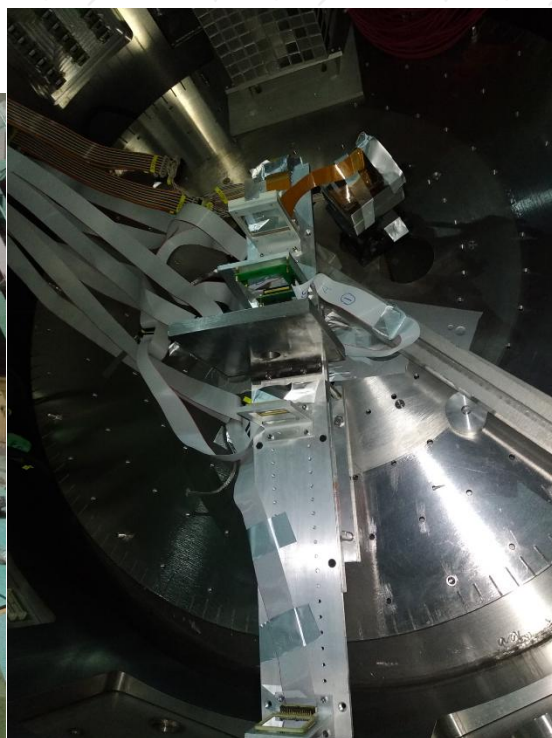
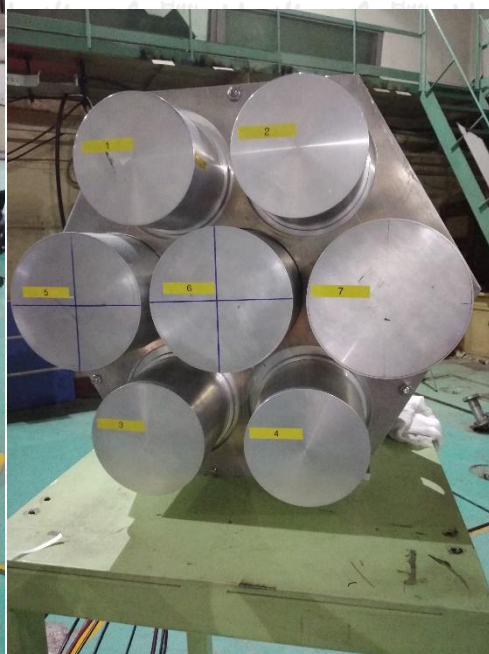
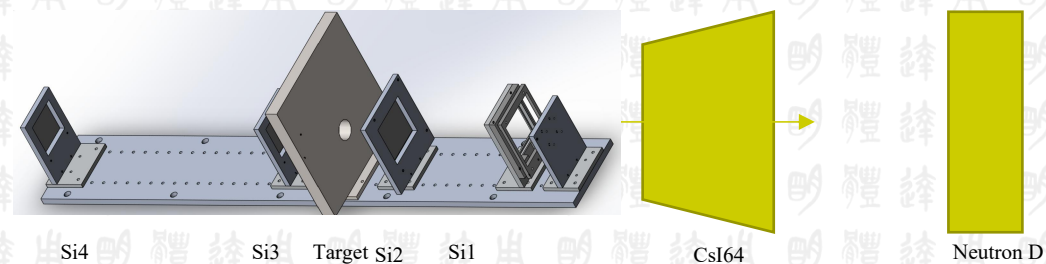
PRL117,182502,2016

准束缚4中子态



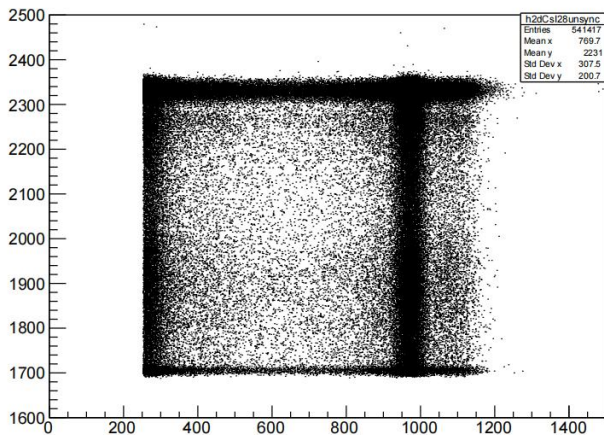
M. Duer et al., nature.606.678 (2022) / J. G. Li et al., PRC 100.054313(2019)

${}^6\text{He}+{}^{208}\text{Pb}$ 反应探测器布局图

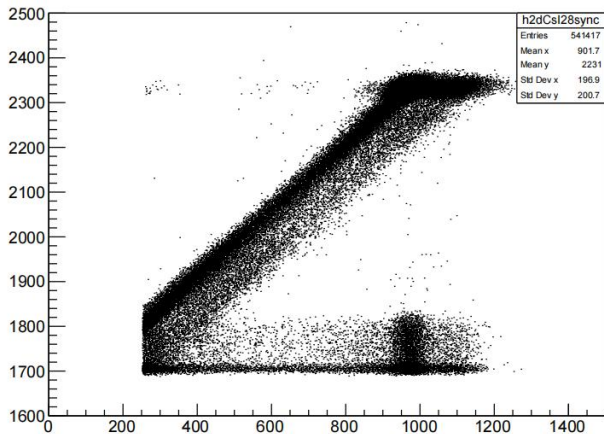


VME与XIA获取系统的同步

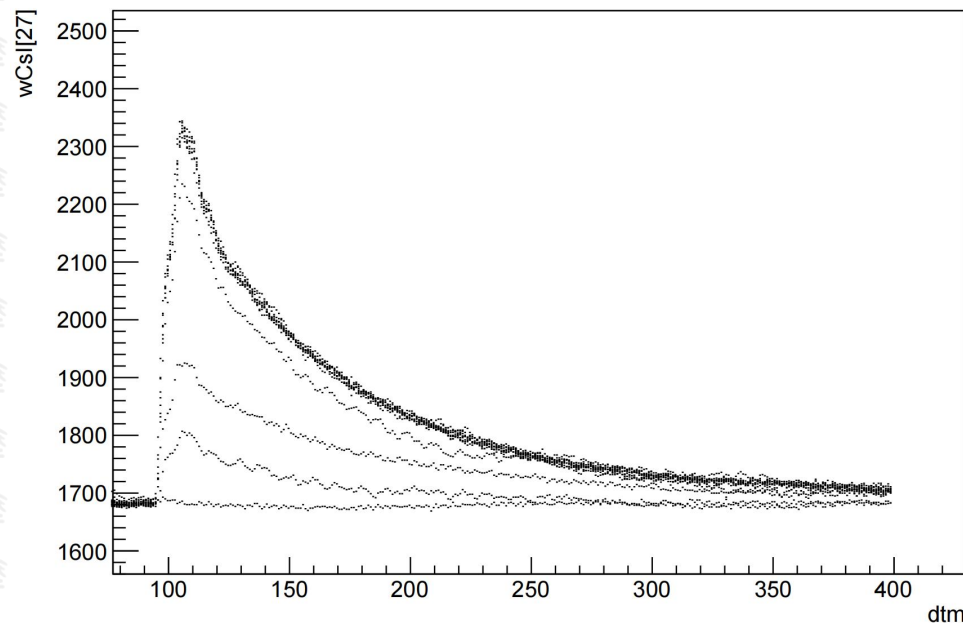
Csl_vme vs Csl_xia uncorrelated events



Csl_vme vs Csl_xia correlated events

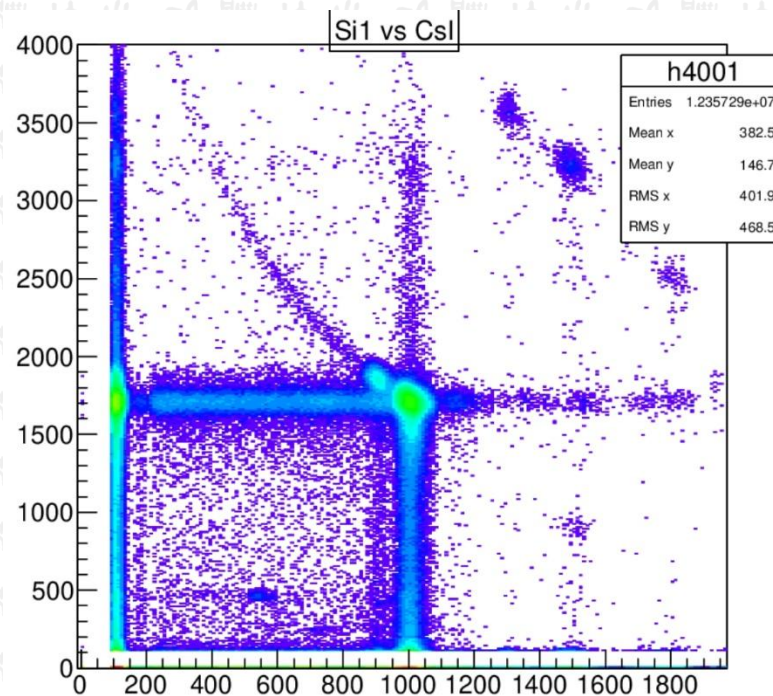
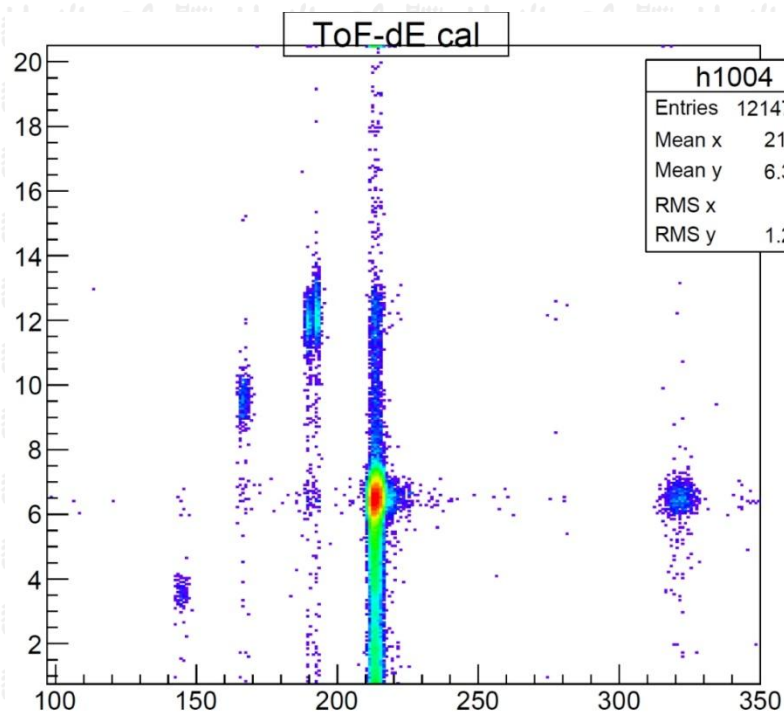


wCsl[27]:dtm





${}^6\text{He}+{}^{208}\text{Pb}$ 实验图谱

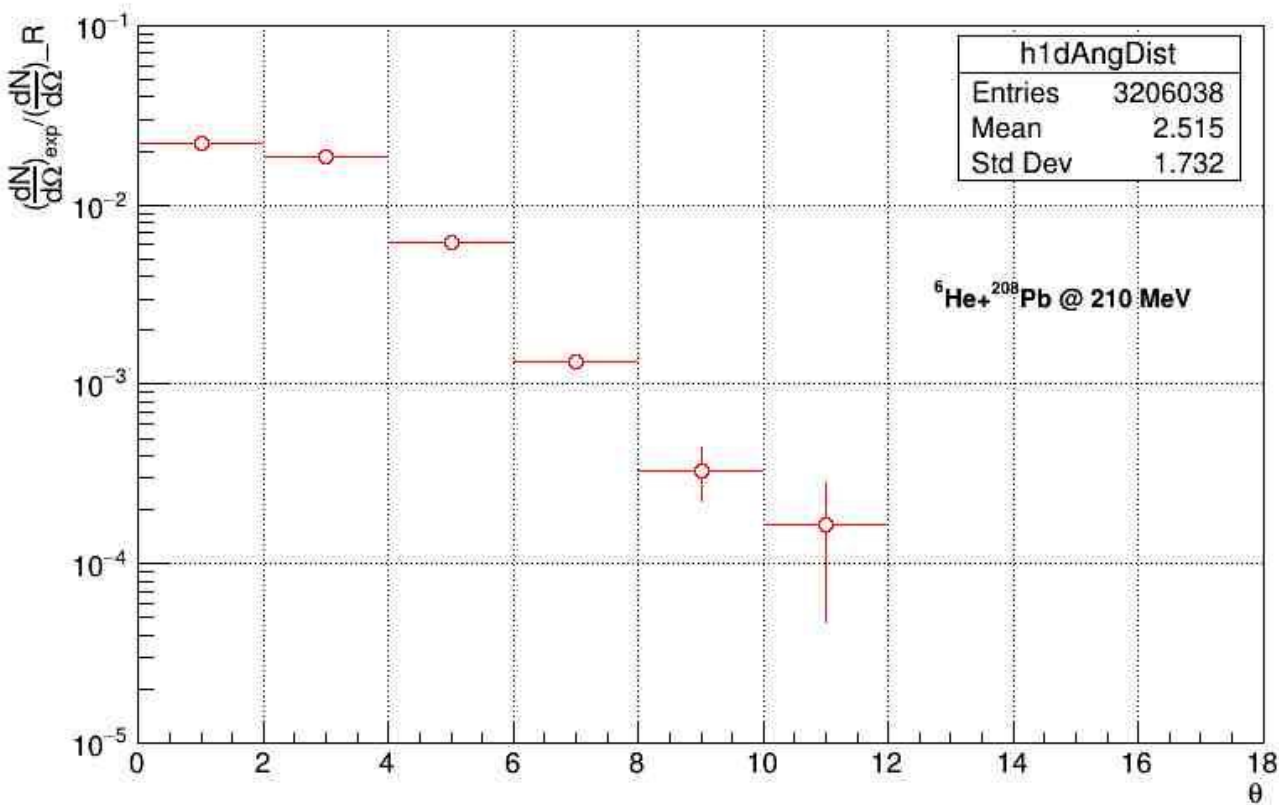


初级束: ${}^{12}\text{C}^{6+}$, 能量为53.98MeV/u, 流强为37enA。

RIBLL1终端顺利调试出 ${}^6\text{He}$ 次级束流, T1和T2符合计数为2700pps, 纯度为98.7%

${}^6\text{He}+{}^{208}\text{Pb}$ 的弹性散射截面初步结果 (10倍库仑位垒)

Angular Distribution Between US and DS





总结与展望

- 中子晕核有明确一致的实验特征和理论解释, 其弹性散射有明显的晕核效应。
- 质子晕(?) ${}^8\text{B}$ 的直接反应机制与中子晕核截然不同。
- 对于质子晕核 ${}^8\text{B}$ 和其他质子滴线核的理解还需要更多的实验和理论:
 - 1) 直接测量 ${}^8\text{B}$ 的电荷半径 (**在线离子束激光谱仪**)
 - 2) 测量不同能区 ${}^8\text{B}$ 破裂碎片p与 ${}^7\text{Be}$ 的关联
- $2n$ 、 $4n$ 等纯中子集团需要更多的实验研究
- t 、 ${}^3\text{He}$ 集团结构可能会是一个新的研究方向

Collaborators

IMP:

Y. Y. Yang(杨彦云), S. L. Jin(金仕纶), P. Ma(马朋), M. R. Huang(黄美容), J. B. Ma(马军兵), F. Fu(付芬), Q. Wang(王琦), D. P. Wu(武大鹏), Q. Hu(胡强), Z. Bai(白真), L. Jin(金磊), J. B. Chen(陈江波), Y. Li(李勇), M. H. Zhao(赵明辉), Y. J. Zhou(周远杰), W. H. Ma(马维虎), J. Chen(陈杰), 余功明, D. B. Patel, 金树亚, 段芳芳 (LZU), 王康, 杨过, 王煜峰(YNU)

M. Wang(王猛), Z. Y. Sun(孙志宇), Z.G.Hu(胡正国), R. F. Chen(陈若富), X. Y. Zhang(张雪荧), X. H. Yuan(袁小华), X. L. Tu(涂小林), Z. G. Xu(徐治国), K. Yue(岳珂), J. D. Chen(陈金达), B. Tang(唐彬), Y. D. Zang(臧永东), Y. H. Zhang(张玉虎), H. S. Xu(徐珊瑚) and G. Q. Xiao(肖国青)

CIAE: C. J. Lin(林承键)研究组; **Peking Univ:** Y. L. Ye (叶沿林) 研究组

Beihang Univ: D. Y. Pang (庞丹阳); **Poland:** N. Keely, K. Rusek

Spain: A. Moro ; **India:** S. Mukerjee

Nanjing Univ./Tongji Univ: Z. Z. Ren(任中洲), C. Xu(许昌), D. D. Ni(倪冬冬), Jin Lei (金磊)

Surrey Univ.: J. A. Tostevin



**Thanks for your
attention !**